

# Pipelining Split Learning in Multi-hop Edge Networks

Wei Wei, *Graduate Student Member, IEEE*, Zheng Lin, *Graduate Student Member, IEEE*, Tao Li, *Graduate Student Member, IEEE*, Xuanheng Li, *Member, IEEE*, and Xianhao Chen, *Member, IEEE*

**Abstract**—To support large-scale model training, split learning (SL) enables multiple edge devices/servers to share the intensive training workload. However, most existing works on SL focus solely on two-tier model splitting. Moreover, while some recent works have investigated the model splitting and placement problems for multi-hop SL, these solutions fail to overcome the resource idleness issue, resulting in significant network idle time. In this work, we propose a pipelined SL scheme by addressing the joint optimization problem of model splitting and placement (MSP) in multi-hop edge networks. By applying pipeline parallelism to SL, we identify that the MSP problem can be mapped to a problem of minimizing the weighted sum of a bottleneck cost function (min-max) and a linear cost function (min-sum). Based on graph theory, we devise a bottleneck-aware shortest-path algorithm to obtain the optimal solution. Besides, given the MSP outcomes, we also derive the closed-form solution to the micro-batch size in the pipeline. Finally, we develop an alternating optimization algorithm of MSP and micro-batch size to solve the joint optimization problem to minimize the end-to-end training latency. Extensive simulations have demonstrated the significant advantages of our algorithm compared to existing benchmarks without pipeline parallelism.

**Index Terms**—Mobile edge computing (MEC), split learning, wireless multi-hop network, pipeline parallelism, combinatorial optimization problem (COP).

## I. INTRODUCTION

Training AI models in the cloud is considered the status quo paradigm, which harnesses the power of large-scale computing units to train powerful AI models. However, considering the fact that most data-generating devices are located at the network edge, cloud training faces critical challenges, including excessive data transmission latency ( $30\times$  to  $100\times$  greater than that experienced in edge environments [1]), high bandwidth costs, scalability issues, and data privacy concerns [2]–[4]. As a result, edge learning becomes an emerging training paradigm that leverages computing capabilities located close to data sources for AI model training [5]. By minimizing privacy exposure and data transmission costs, edge learning is expected to play a vital role in various mission-critical applications

such as healthcare [6]–[8], industrial automation [9], [10], and smart-city operations [11], [12], where directly sharing personal, enterprise, or government data is bandwidth-costly or prohibited by data protection regulations [13].

However, as AI models expand in size, it becomes increasingly challenging and time-consuming to train advanced AI models on a *single* edge server [14]; for example, state-of-the-art on-device models, such as TinyLLaMa, consist of over 1.1 billion parameters [15], [16], impose substantial training workload that can easily overwhelm an edge server, resulting in *excessive training latency* and *memory overflow*. To tackle the above challenges, *multi-hop* split learning (SL) can be employed to facilitate the training of giant models at the network edge [17]–[19]. The initial motivation behind vanilla SL is to train a model in a privacy-enhancing manner, which is achieved by splitting a model between a server and a user for training [17], [20]. By extending it to multi-hop SL, a large AI model can be partitioned into multiple submodels and distributed across geographically dispersed edge servers. In practice, these edge servers can either be enterprise private edge servers or public edge servers co-located with base stations in mobile networks. Regardless of their types, when forming a mesh of computing facilities, they constitute a distributed yet powerful computing infrastructure for large-scale model training [21]. As shown in Fig. 1(a), splitting a VGG-16 model among multiple edge servers can significantly reduce the training latency. Moreover, model splitting can also decrease the memory demands per server, which is equally crucial as the memory space is one of the most scarce resources on edge servers/devices.

While multi-hop SL provides a promising solution to train a large-sized model at the network edge, implementing this framework encounters two major difficulties. The first difficulty comes from *resource heterogeneity*. Since model training in edge networks involves servers with significantly heterogeneous computing, memory, and communication capabilities [16], [24], inappropriate model splitting and placement can result in bottleneck servers/links, leading to intolerable latency. For instance, a typical edge server might have a GPU like the NVIDIA GeForce RTX 4090 with 82 TFLOPS, while an edge device like the Raspberry Pi 4 performs at just 13.5 GFLOPS, leading to a performance difference of nearly four orders of magnitude [25], [26]. The second difficulty stems from *resource idleness*. Given the interdependency of forward and backward passes in multi-hop SL, the majority of servers/links sit idle during training, resulting in excessive latency. This phenomenon becomes even severer as the number

The work was supported in part by the Research Grants Council of Hong Kong under Grant 27213824 and in part by HKU IDS Research Seed Fund under Grant IDS-RSF2023-0012. (*Corresponding author: Xianhao Chen*)

Wei Wei, Zheng Lin, Tao Li and Xianhao Chen are with the Department of Electrical and Electronic Engineering, University of Hong Kong, Pok Fu Lam, Hong Kong SAR, China. Xianhao Chen is also with HKU Musketeers Foundation Institute of Data Science, University of Hong Kong, Pok Fu Lam, Hong Kong SAR, China. (e-mail: weiwei@eee.hku.hk; linzheng@eee.hku.hk; lthku999@connect.hku.hk; xchen@eee.hku.hk).

Xuanheng Li is with the School of Information and Communication Engineering, Dalian University of Technology, Dalian 116023, China (e-mail: xhli@dlut.edu.cn).

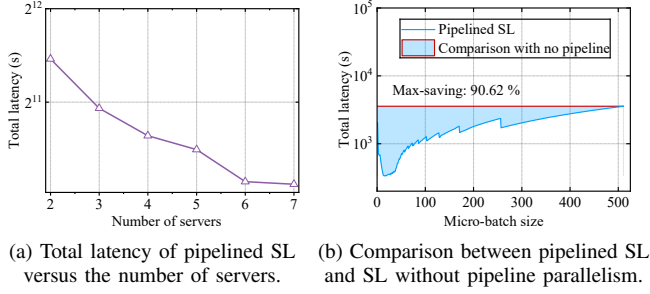


Fig. 1: Total latency in pipelined SL, which trains a VGG-16 model [22] on the CIFAR-10 dataset [23] under IID settings. The computing capability of each edge server (NVIDIA GeForce RTX 4090) is uniformly distributed within [1, 10] TFLOPS. The total available bandwidth ranges from 10 MHz to 200 MHz.

of hops increases, hampering the scalability of training large-sized models in an edge computing network.

Despite the fact that resource optimization of multi-hop SL can significantly influence its system performance, none of the existing schemes address resource heterogeneity and resource idleness as a whole. On the one hand, prior works on distributed training usually consider multi-GPU or multi-server training in cloud centers, assuming *homogeneous* GPU configurations and *identical* inter-GPU communication latency [27], [28]. As a result, model splitting and placement are normally not optimized therein. However, model splitting and placement under heterogeneous communication-computing resource constraints are essential considerations in edge networks. On the other hand, a few recent works have addressed model splitting and placement in edge networks by considering heterogeneous communication and computing capabilities. Nevertheless, since these works mostly focus on multi-hop split inference problems [29]–[31] or consider a single batch of training data successively going through the forward and backward passes, none of them mitigate resource idleness issues, as only one server or communication link can be active at a time during the process.

To address all the above issues, in this paper, we propose a pipelined SL scheme as our answer to effective implementations of multi-hop SL in edge networks. Unlike existing multi-hop split learning or inference schemes [29], [32]–[34], our proposed framework involves an essential pipeline parallelism procedure, which divides a training dataset into multiple micro-batches for parallel processing across edge servers [35]. As illustrated in Fig. 1(b), compared with SL without pipeline parallelism, the proposed scheme can considerably reduce training latency by mitigating network idleness upon forward and backward passes. Based on this framework, we study the optimization problem of model splitting and placement (MSP) for pipelined SL in edge networks with limited communication-computing resources. To minimize the end-to-end latency, we discern that the resulting MSP problem can be mapped to a problem of minimizing the weighted sum of a bottleneck cost function (min-max) and a linear

cost function (min-sum), which can be solved exactly through graph theory. Specifically, the linear cost stems from the latency for the first micro-batch to be finished, whereas the bottleneck cost comes from the pipeline process. A block coordinate descent (BCD) is then developed to solve the joint problem by also incorporating the optimization of micro-batch size. Our key contributions are summarized below.

- To our knowledge, this is the first work that formulates a unified optimization framework that jointly determines model splitting & placement (MSP) and micro-batch size for pipelined split learning in multi-hop edge networks, with the explicit goal of minimizing end-to-end training latency under heterogeneous communication, computation, and memory constraints.
- We show that the resultant MSP subproblem can be mapped to a problem with combined min-max and min-sum objective. By mapping the problem into a graph, we develop a *bottleneck-aware shortest-path* algorithm to obtain the optimal solution.
- Given the fixed MSP results, we obtain the optimal closed-form solution to micro-batch size for the micro-batching subproblem. Subsequently, we devise a BCD-based method to obtain an efficient sub-optimal solution to the joint optimization problem.
- Simulations have shown the significant advantages of our approaches compared with existing multi-hop SL benchmarks.

The remainder of this paper is organized as follows. Section II introduces related work. Section III elaborates on the system model. We formulate the optimization problem in Section IV, develop the corresponding solution approach in Section V, and provide the simulation results in Section VI. Finally, we conclude the paper in Section VII.

## II. RELATED WORK

Several existing works have studied multi-hop split machine learning, including split inference and learning, under computing, memory, and/or communication constraints. Kang et al. [32], [36]–[39] first exploit the potential of distributing DNN inference between cloud servers and mobile devices to optimize latency, energy consumption, and throughput. Specifically, a lightweight scheduler has been introduced to partition DNN tasks in cloud-edge systems dynamically. In [29], a scheme called HiveMind has been devised to facilitate multi-hop split inference in 5G networks. By reformulating the model splitting problem as a min-cost graph search, HiveMind efficiently adapts to real-time network dynamics, significantly reducing signaling overhead. Moreover, Hu et al. [33] optimally partition DNNs between edge and cloud computing based on dynamic network conditions, which addresses the computational and transmission trade-offs. Xiao et al. [34] propose an efficient multi-hop edge inference, which allows mobile devices to dynamically select the optimal partition point of deep learning models and choose collaborative edge servers based on real-time conditions. However, although split inference and SL bear similarities, some significant differences exist. Particularly, split inference often takes one data sample

at a time rather than processing a batch of training data. This implies that pipeline parallelism, considered essential for the SL process, does not appear in split inference. Mathematically, our work will show that the latency minimization problem of pipelined SL turns out to be a min-max-min-sum problem, as the total latency accounts when the first micro batch enters the multi-hop networks until the last micro batch comes out.

Pipeline parallelism is a widely studied topic in distributed training [27], [40], [41]. The basic idea is to make computing and communication “interleaved” across different devices (often GPUs) to reduce idle time. PipeDream [28] uses a one forward pass followed by one backward pass (1F1B) scheduling approach to interleave forward pass (FP) and backward pass (BP) and addresses weight staleness issues arising from asynchronous backward updates. GPipe [27] uses synchronous stochastic gradient descent (SGD) and divides mini-batches into smaller micro-batches to minimize bubble time. Synchronization happens at the end of each mini-batch by aggregating gradients from all micro-batches. Moreover, Chimera [40] employs bidirectional pipelines for efficient training of large-scale neural networks, which minimizes the number of pipeline bubbles by up to 50% compared to GPipe. Nevertheless, this line of research does not consider the MSP problem under heterogeneous communication-computing constraints – a feature that edge networks possess.

Multi-hop SL has also been investigated in some literature. In [42], RNN is partitioned into sub-models and deployed on multiple mobile devices for training via inter-device communication. DAPPLE [43] combines data and pipeline parallelism for synchronous training of large DNN models. It features a dynamic programming-based planner to split and place model layers on devices. In [44], Tian et al. devise a model splitting and neural architecture search framework for SL in a mesh network. However, pipeline parallelism has not been considered in these works. The most related work is [45], which proposes a parallel SL framework addressing multi-hop MSP problem. Nevertheless, this framework does not account for communication latency in the MSP optimization problem, overlooking the effects of network topology and bandwidth. In addition, it employs a fixed batch size throughout training without taking advantage of joint batching and MSP optimization. To our best knowledge, our paper presents the first pipelined SL framework to address the MSP optimization under *communication-computing* resource constraints.

### III. SYSTEM MODEL

#### A. Architecture Overview

Fig. 2 illustrates a multi-hop SL framework based on pipeline scheduling with multiple edge nodes including clients and edge servers. In practice, the next-generation user plane function (UPF) enables the routing of application traffic among users and mobile edge computing (MEC) servers associated with different network entities, thereby facilitating a multi-hop SL paradigm [29]. Each edge server, e.g., an MEC node in the platform, can execute FP and BP model trainings. Moreover, we consider a scenario where  $N$  edge servers  $S = \{1, 2, \dots, N\}$  participate in the multi-hop SL system

TABLE I: Summary of Key Notations.

Notations	Descriptions
$I$	The number of layers of a neural network
$K$	The number of submodels
$N$	The number of edge servers
$M$	The number of clients
$x_{ik}$	The cutting strategy, where $x_{ik} = 1$ represents the last layer of the $k$ -th submodel with the index $i$ and $x_{ik} = 0$ otherwise
$y_{kn}$	The placement strategy, where $y_{kn} = 1$ if the $k$ -th submodel is deployed to client/server $n$ and 0 otherwise
$B_m$	The number of total data samples from client $m$
$B$	The number of total data samples in the mini-batch
$b$	The number of server-side data samples in a micro-batch
$b_m$	The number of client-side data samples in a micro-batch
$D_k$	The data size of activations
$D'_k$	The data size of activations' gradients
$\eta_k$	The memory cost to process the $k$ -th submodel
$M_n$	The maximum GPU memory of client/server $n$
$P$	The number of parameters
$W_{nn'}$	The channel bandwidth between $n$ and $n'$
$N_0$	The noise power
$p_n$	The transmit power of client/server $n$
$d_{nn'}$	The distance between $n$ and $n'$
$\gamma$	The path loss exponent
$r_{nn'}$	The achievable data rate over wireless link between $n$ and $n'$
$f_n$	The computing capability of client/server $n$
$\kappa_n$	The computing intensity of client/server $n$
$w_i$	The computing workload per data sample of FP for the first $i$ -th layers
$\rho_i$	The computing workload per data sample of BP for the first $i$ -th layers
$\varphi_i$	The size of activations of the $i$ -th layer
$\phi_i$	The size of activations' gradients of the $i$ -th layer

to process a neural network with  $I$  layers cooperatively. We define the overall set of nodes as  $\mathcal{N}$  and denote the set of clients as  $\mathcal{N}_c$ , where  $\mathcal{N}_c \subset \mathcal{N}$ . Next, we define the decision variables, i.e., model split matrix and model placement matrix as follows,

- Model split matrix  $\mathbf{x} = \{x_{ik} | i \in [1, I], k \in [1, K-1]\}$ :  $x_{ik} = 1$  represents that the last layer of the  $k$ -th submodel is layer  $i$  and  $x_{ik} = 0$  otherwise.
- Model placement matrix  $\mathbf{y} = \{y_{kn} | k \in [1, K], n \in \mathcal{N}\}$ : For edge server  $n \in \mathcal{N} \setminus \mathcal{N}_c$ ,  $y_{kn} = 1$  denotes that the  $k$ -th submodel ( $k \in [2, K]$ ) is deployed on server  $n$ , and  $y_{kn} = 0$  otherwise. For client  $n \in \mathcal{N}_c$ , we enforce  $y_{kn} = 1$ , indicating that the first submodel ( $k = 1$ ) should be deployed on the client side for preventing raw data transmissions to edge servers.

Herein,  $K$  denotes the maximum number of submodels after model splitting. Notably, the copies of the first submodel ( $k = 1$ ) are placed on  $M$  clients  $\mathcal{C} = \{1, 2, \dots, M\}$ . In each training round, client  $m$  processes mini-batch  $B_m$  of data samples. Assume that the clients connect to an access edge server, the edge server draws mini-batch  $B = \sum_{m=1}^M B_m$  of data samples for split training based on mini-batch SGD. As shown in Fig. 2, the mini-batch  $B$  will be divided into smaller *micro-batch*  $b$  for pipeline parallelism, thus enabling parallel process across edge nodes. Besides, we assume that the average data rate between servers and the network topology remain unchanged within each training round. Moreover, we mainly focus on one training round while omitting the training round

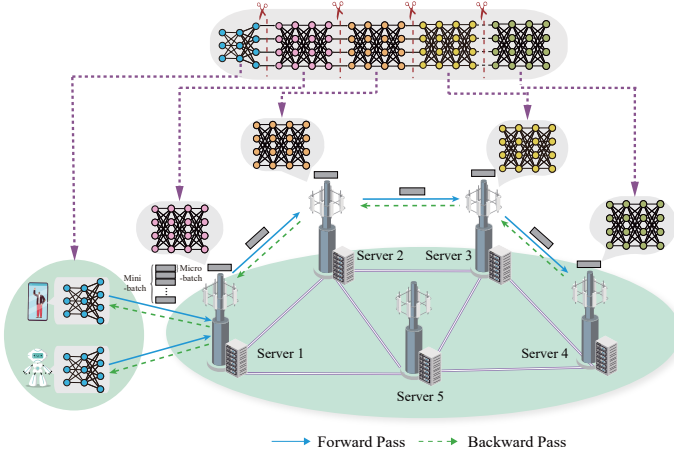


Fig. 2: Pipelined split learning in multi-hop edge networks.

index. Our optimization goal is to train the neural network with the minimum end-to-end latency by jointly optimizing the cut layers, submodel placement, and micro-batching. The training process in each training round is elaborated as follows.

### B. FP & Activation Transmissions

1) *The FP process*: In the FP process, submodel  $k$  (placed on a client or a client or an edge server) receives the activations of the prior submodel (if any) as the inputs, performs FP to produce the output activations, and feeds the activations to the next submodel, which is placed on another edge server. The process terminates once the computation of all layers of the entire neural network is finished. Without loss of generality, we assume each client  $m$  draws  $b_m$  data samples and the first server draws a micro-batch of  $b = \sum_{m=1}^M b_m$  data samples to execute the FP process. Specifically, we arrange  $\lfloor \frac{b}{M} \rfloor$  data samples to each of the first  $M - 1$  clients and allocate the remaining  $b - (M - 1) \lfloor \frac{b}{M} \rfloor$  data samples to the  $M$ -th client, which is expressed by

$$b_m = \begin{cases} \lfloor b/M \rfloor, & 1 \leq m \leq M - 1, \\ b - (M - 1) \lfloor b/M \rfloor, & m = M. \end{cases} \quad (1)$$

In this way, the forward pass latency of edge server  $n$  for processing the  $k$ -th submodel can be expressed as

$$t_{k,n}^F(b, \mathbf{x}) = \begin{cases} b_m \kappa_n \delta_{kn}^F(\mathbf{x}) / f_n + t_0^c, & \forall n \in \mathcal{N}_c, \\ b \kappa_n \delta_{kn}^F(\mathbf{x}) / f_n + t_0^s, & \forall n \in \mathcal{N} \setminus \mathcal{N}_c, \end{cases} \quad (2)$$

where  $\mathbf{x}$  is the collection of  $x_{ik}$ ,  $f_n$  denotes the computing capability (in CPU/GPU frequency) of server  $n$ ,  $\kappa_n$  represents the computing intensity [46],  $t_0^c$  and  $t_0^s$  are coefficients related to initialization and model loading, and

$$\delta_{kn}^F(\mathbf{x}) = \begin{cases} \sum_{i=1}^I x_{ik} w_i, & \forall n \in \mathcal{N}_c, k = 1, \\ \sum_{i=1}^I (x_{ik} - x_{i(k-1)}) w_i, & \forall n \in \mathcal{N} \setminus \mathcal{N}_c, k \in [2, K], \end{cases} \quad (3)$$

with  $w_i$  being the computing workload per data sample of FP for the first  $i$ -th layers.

2) *Activations transmission*: After the  $k$ -th submodel completes the FP process on the client  $m$  or edge server  $n$ , the host client/server transmits the activations to the subsequent server  $n'$  over a wired/wireless channel. For instance, if the connection is wireless (e.g., using 5G wireless backhaul), the achievable data rate  $r_{nn'}$  over the link is given by

$$r_{nn'} = W_{nn'} \cdot \log \left( 1 + (d_{nn'})^{-\gamma} p_n / N_0 \right), \quad \forall n \in \mathcal{N}, \forall n' \in \mathcal{N}, \quad (4)$$

where  $p_n$  is the transmit power,  $d_{nn'}$  denotes the distance between edge nodes  $n$  and  $n'$ ,  $W_{nn'}$  is the channel bandwidth,  $\gamma$  is the path loss exponent, and  $N_0$  is the noise power. Besides, the data size  $D_k(\mathbf{x}, b)$  of the activations generated by the  $k$ -th submodel is defined as

$$D_k(\mathbf{x}, b) = \begin{cases} b_m \sum_{i=1}^I x_{ik} \varphi_i, & k = 1, \\ b \sum_{i=1}^I x_{ik} \varphi_i, & \forall k \in [2, K - 1], \end{cases} \quad (5)$$

where  $\varphi_i$  stands for the size of activations of at layer  $i$ . Thus, the communication latency can be expressed as

$$t_{k,nn'}^F = D_k(\mathbf{x}, b) / r_{nn'}, \quad \forall n, n' \in \mathcal{N}, \forall k \in [1, K - 1]. \quad (6)$$

### C. BP & Activations' Gradients Transmission

1) *The BP process*: After a micro-batch finishes the FP process, the BP process begins at the last layer and moves backward to the very first layer. Each submodel  $k$  ( $k \neq K$ ) receives the activations' gradients of subsequent submodel as the inputs, performs computations, and feeds the results to the preceding submodel. The process terminates once the computation of all layers is finished. The backward pass latency  $t_{k,n}^B(b, \mathbf{x})$  on server  $n$  for processing the  $k$ -th submodel is expressed as

$$t_{k,n}^B(b, \mathbf{x}) = \begin{cases} t_1^c, & \forall n \in \mathcal{N}_c, 0 < b_m \leq b_{th}^c, \\ t_1^s, & \forall n \in \mathcal{N} \setminus \mathcal{N}_c, 0 < b \leq b_{th}^s, \\ (b_m - b_{th}^c) \kappa_n \delta_{kn}^B(\mathbf{x}) / f_n + t_1^c, & \forall n \in \mathcal{N}_c, b_{th}^c < b_m \leq B, \\ (b - b_{th}^s) \kappa_n \delta_{kn}^B(\mathbf{x}) / f_n + t_1^s, & \forall n \in \mathcal{N} \setminus \mathcal{N}_c, b_{th}^s < b \leq B, \end{cases} \quad (7)$$

with

$$\delta_{kn}^B(\mathbf{x}) = \begin{cases} \sum_{i=1}^I x_{ik} \rho_i, & \forall n \in \mathcal{N}_c, k = 1, \\ \sum_{i=1}^I (x_{ik} - x_{i(k-1)}) \rho_i, & \forall n \in \mathcal{N} \setminus \mathcal{N}_c, k \in [2, K], \end{cases} \quad (8)$$

where  $\rho_i$  is the computing workload per data sample of BP for the first  $i$ -th layers, and the coefficients  $b_{th}^c$ ,  $b_{th}^s$ ,  $t_1^c$  and  $t_1^s$  are determined by specific DNN models and hardware [47].

2) *Transmissions of activations' gradients*: When the BP process of a submodel is completed, activations' gradients at the cut layer will be transmitted through the communication links. The data size  $D'_k(\mathbf{x}, b)$  of the activations' gradients generated by the  $k$ -th submodel is expressed as

$$D'_k(\mathbf{x}, b) = \begin{cases} b_m \sum_{i=1}^I x_{ik} \phi_{(i+1)}, & k = 1, \\ b \sum_{i=1}^I x_{ik} \phi_{(i+1)}, & \forall k \in [2, K-1], \end{cases} \quad (9)$$

where  $\phi_{(i+1)}$  stands for the size of activations' gradients at cut layer  $i+1$ . Thus, the communication latency between node  $n'$  and  $n$  for the  $k$ -th submodel can be expressed as [48]

$$t_{k,n'n}^B = D'_k(\mathbf{x}, b)/r_{n'n}, \quad \forall n, n' \in \mathcal{N}, \quad \forall k \in [1, K-1]. \quad (10)$$

#### D. Memory Consumption

In multi-hop SL, it is crucial to avoid out-of-memory failures during model training [49]. The required memory space to process the  $k$ -th submodel is denoted by

$$\eta_k(\mathbf{x}, b) = \begin{cases} b_m \sum_{i=1}^I x_{ik} (\tilde{\varphi}_i + \tilde{\phi}_i + \tilde{\sigma}_i + \beta_i), & k = 1, \\ b \sum_{i=1}^I (x_{ik} - x_{i(k-1)}) (\tilde{\varphi}_i + \tilde{\phi}_i + \tilde{\sigma}_i + \beta_i), & k \in [2, K], \end{cases} \quad (11)$$

where  $\tilde{\varphi}_i = \sum_{i'=1}^i \varphi_{i'}$  and  $\tilde{\phi}_i = \sum_{i'=1}^i \phi_{i'}$  represent the cumulative sum of the data size of activations and activations' gradients for first  $i$  layers of neural network,  $\tilde{\sigma}_i$  is the data size of the optimizer state for the first  $i$  layers of neural network, depending on the choice of the optimizer (e.g. SGD, Momentum, and Adam), and  $\beta_i$  is the parameter size of the first  $i$  layers.

#### IV. PROBLEM FORMULATION

In our SL design, the core innovation lies in pipelining successive micro-batches under heterogeneous communication-computing resource constraints, thereby mitigating resource heterogeneity and idleness issues. However, this *pipeline process in edge networks* also leads to a challenging optimization problem different from previous works [29], [45]. Specifically, we aim to minimize the total training latency of pipelined SL, which contains 1) latency  $T_f(\mathbf{x}, \mathbf{y}, b)$  for the first micro-batch to complete the FP and BP processes, and 2) the pipeline latency for the remaining micro-batches to finish the processes. For the first part,  $T_f(\mathbf{x}, \mathbf{y}, b)$  is given by

$$T_f(\mathbf{x}, \mathbf{y}, b) = \max_{n \in \mathcal{N}_c} \{t_{1,n}^F(b, \mathbf{x}) + \sum_{n'=1}^N y_{2n'} t_{1,n'n}^F(\mathbf{x}, b)\} + \sum_{k=2}^K \sum_{n=1}^N y_{kn} [t_{k,n}^F(b, \mathbf{x}) + t_{k,n}^B(b, \mathbf{x})] + \sum_{n=1}^N \sum_{n'=1}^N \left\{ \sum_{k=2}^{K-1} y_{kn} y_{(k+1)n'} \right.$$

$$\left. t_{k,nn'}^F(\mathbf{x}, b) + \sum_{k=2}^{K-1} y_{(k+1)n'} y_{kn} t_{k,n'n}^B(\mathbf{x}, b) \right\} + \max_{n \in \mathcal{N}_c} \{t_{1,n}^B(b, \mathbf{x}) + \sum_{n'=1}^N y_{2n'} t_{1,n'n}^B(\mathbf{x}, b)\}, \quad (12)$$

where  $\mathbf{x}$  is the collection of  $x_{ik}$  and  $\mathbf{y}$  is the collection of  $y_{kn}$ . The four terms in (12) correspond to the FP and activation transmissions on clients, the FP and BP on edge servers, the communication latency among edge servers, and the BP and activations' gradients transmissions on clients, respectively.

Considering multiple micro-batches to be processed, we assume that "FP & activations transmission" and "BP & activations' gradients transmission" are executed in *pipeline*. To derive the pipeline latency, we need to calculate the *difference of completion time of two consecutive micro-batches*, which can be derived from

$$T_i(\mathbf{x}, \mathbf{y}, b) = \max \left\{ \max_{k \in [2, K-1]} \left\{ \sum_{n=1}^N y_{kn} t_{k,n}^F(b, \mathbf{x}), \sum_{n=1}^N y_{kn} t_{k,n}^B(b, \mathbf{x}), \sum_{n=1}^N \sum_{n'=1}^N y_{kn} y_{(k+1)n'} t_{k,nn'}^F(\mathbf{x}, b), \sum_{n=1}^N \sum_{n'=1}^N y_{kn} y_{(k+1)n'} t_{k,n'n}^B(\mathbf{x}, b) \right\}, \right. \\ \left. \max_{n \in \mathcal{N}_c} \{t_{1,n}^F(\mathbf{x}) + \sum_{n'=1}^N y_{2n'} t_{1,n'n}^F(\mathbf{x}, b)\}, \max_{n \in \mathcal{N}_c} \{t_{1,n}^B(\mathbf{x}) + \sum_{n'=1}^N y_{2n'} t_{1,n'n}^B(\mathbf{x}, b)\} \right\}. \quad (13)$$

Intuitively,  $T_i(\mathbf{x}, \mathbf{y}, b)$  is determined by the *bottleneck latency* over the multi-hop systems, which is equal to the maximum latency over any computing server or communication link. Moreover, the batch per training round with  $B$  data samples needs to be transmitted  $\lceil B/b \rceil$  times. Thus, the total latency  $L_t(\mathbf{x}, \mathbf{y}, b)$  can be formulated as

$$L_t(\mathbf{x}, \mathbf{y}, b) = T_f(\mathbf{x}, \mathbf{y}, b) + \lceil (B-b)/b \rceil T_i(\mathbf{x}, \mathbf{y}, b), \quad (14)$$

where the second term is the pipeline latency. In the multi-hop SL system, *the overarching goal is to jointly optimize the cutting layers, model placement, and micro-batch size to minimize the total latency  $L_t(\mathbf{x}, \mathbf{y}, b)$* . Thus, the optimization problem can be formulated as

$$\begin{aligned} \mathcal{P}1 : & \min_{\{\mathbf{x}, \mathbf{y}, b\}} L_t(\mathbf{x}, \mathbf{y}, b) \\ \text{s.t.} \quad & \text{C1: } x_{ik} \in \{0, 1\}, \quad \forall i \in [1, I], \quad k \in [1, K-1], \\ & \text{C2: } y_{kn} \in \{0, 1\}, \quad \forall k \in [1, K], \quad n \in \mathcal{N}, \\ & \text{C3: } b \in \{1, 2, \dots, B\}, \\ & \text{C4: } \sum_{i=1}^I x_{ik} = 1, \quad \forall k \in [1, K-1], \\ & \text{C5: } \sum_{i=1}^{I'} x_{ik} \leq \sum_{i=1}^{I'} x_{i(k-1)}, \quad \forall k \in [2, K-1], \quad I' \in [1, I], \\ & \text{C6: } \sum_{n=1}^N y_{kn} = 1, \quad \forall k \in [2, K], \end{aligned}$$

$$\begin{aligned}
\text{C7 : } & 0 \leq m_1(x_{i1}, b) \leq M_n, \forall n \in \mathcal{N}_c, \\
\text{C8 : } & 0 \leq \sum_{k=2}^K y_{kn} m_k(x_{ik}, b) \leq M_n, \forall n \in \mathcal{N} \setminus \mathcal{N}_c.
\end{aligned} \tag{15}$$

Constraints C1 and C2 ensure that model splitting and placement are binary variables. Constraint C3 means that the micro-batch size should be no more than the mini-batch size  $B$ . Since gradient updating will be made after each mini-batch,  $B$  is a hyperparameter that can be appropriately chosen based on learning efficiency. Other constraints are explained below.

- Cutting layer constraints: C4 ensures the uniqueness of cut layer selection for each submodel. Notice that C4 does not exclude the case that different submodels can select the same cut layer  $i$ , implying that the model can be split into less than  $K$  parts, where  $K \leq I$  is a predetermined constant. This is because splitting models may not always lead to shorter latency due to extra communication latency. Furthermore, the layer dependency Constraint C5 ensures that the neural network layers are in order, i.e., the index of the cut layer of the  $(k-1)$ -th submodel is no greater than that of the  $k$ -th submodel (the equality holds when there is an “empty” submodels).
- The placement constraint: C6 ensures that each submodel can be placed on one edge node. It is noted that submodel  $k$  can be “empty” as alluded to earlier.
- The GPU memory constraint: Constraint C7 and Constraint C8 ensure that the memory cost to process the  $k$ -th submodel is no more than the maximum GPU memory capacity  $M_n$ .

The optimization Problem  $\mathcal{P}1$  turns out to be a nonlinear integer programming (NILP) problem since it involves the minimization of a non-linear function  $L_t(\mathbf{x}, \mathbf{y}, b)$  and a non-linear Constraint C7. In what follows, we show Problem  $\mathcal{P}1$  is NP-hard.

**Proposition 1.** *The latency minimization Problem  $\mathcal{P}1$  is NP-hard.*

*Proof.* Problem  $\mathcal{P}1$  can be decomposed into three sub-problems, namely layer splitting, model placement, and micro-batching. When fixing the other two sub-problems, the placement sub-problem is a knapsack problem [50] which is NP-hard. Consequently, Problem  $\mathcal{P}1$  is NP-hard.  $\square$

## V. SOLUTION APPROACH

In this section, we first reformulate Problem  $\mathcal{P}1$  and analyze the computation complexity of the latency minimization problem. Then, we decompose the problem into two subproblems, i.e., the MSP problem and the micro-batching problem. Given fixed MSP results, we derive the optimal solution to the micro-batching subproblem. Moreover, we identify that the MSP problem is a problem with a combined min-max min-sum objective function, which can be efficiently solved based on graph theory.

### A. Problem Reformulation

The optimization objective of Problem  $\mathcal{P}1$  is nonlinear and contains the ceil function. To tackle this challenge, we

introduce an auxiliary variable  $T_1$  subject to  $T_1 \geq T_i(\mathbf{x}, \mathbf{y}, b)$  and function  $\xi(b) = \lceil (B - b/b) \rceil$ .  $\mathcal{P}1$  is then converted into

$$\mathcal{P}2 : \min_{\{\mathbf{x}, \mathbf{y}, b, T_1\}} T_f(\mathbf{x}, \mathbf{y}, b) + \underbrace{\lceil (B - b/b) \rceil}_{\xi(b)} \cdot T_1$$

s.t. C1 - C8,

$$\begin{aligned}
\text{C9 : } & \sum_{k=2}^K y_{kn} t_{k,n}^F(b, \mathbf{x}) \leq T_1, \forall n \in \mathcal{N} \setminus \mathcal{N}_c, \\
\text{C10 : } & t_{1,n}^F(b, \mathbf{x}) \leq T_1, \forall n \in \mathcal{N}_c, \\
\text{C11 : } & b \sum_{k=2}^{K-1} y_{kn} y_{(k+1)n'} \sum_{i=1}^I x_{ik} \varphi_i / r_{nn'} \leq T_1, \\
& \forall n, n' \in \mathcal{N} \setminus \mathcal{N}_c, \\
\text{C12 : } & b_m \sum_{i=1}^I x_{i1} \varphi_i / r_{nn'} \leq T_1, \\
& \forall n \in \mathcal{N}_c, n' \in \mathcal{N} \setminus \mathcal{N}_c, \\
\text{C13 : } & \sum_{k=2}^K y_{kn} t_{k,n}^B(b, \mathbf{x}) \leq T_1, \forall n \in \mathcal{N} \setminus \mathcal{N}_c, \\
\text{C14 : } & t_{k,n}^B(b, \mathbf{x}) \leq T_1, \forall n \in \mathcal{N}_c, \\
\text{C15 : } & b \sum_{k=2}^{K-1} y_{kn} y_{(k+1)n'} \sum_{i=1}^I x_{ik} \phi_{(i+1)} / r_{nn'} \leq T_1, \\
& \forall n, n' \in \mathcal{N} \setminus \mathcal{N}_c, \\
\text{C16 : } & b_m \sum_{i=1}^I x_{i1} \phi_{(i+1)} / r_{nn'} \leq T_1, \\
& \forall n \in \mathcal{N}_c, n' \in \mathcal{N} \setminus \mathcal{N}_c,
\end{aligned} \tag{16}$$

Specifically, the additional Constraints C9-C16 are established according to Eq. (13). The transformed Problem  $\mathcal{P}2$  is equivalent to the original Problem  $\mathcal{P}1$ , as the optimal solution  $T_1^*$  obtained from Problem  $\mathcal{P}2$  should meet  $T_1^* = T_i(\mathbf{x}, \mathbf{y}, b)$ .

### B. Complexity Analysis

If we take the brute-force approach and examine all possible layer splitting, model placement and micro-batching options to tackle Problem  $\mathcal{P}2$ , then it requires calculating the latency for all  $\sum_{k=2}^N B \binom{I-1}{k-1} k! \binom{N}{k}$  options! For example, given  $B = 256$ , the VGG-16 model to be split and deployed on no more 5 edge nodes have approximately  $5.76 \times 10^7$  options. Examining such a huge number of options requires significant processing time. Moreover, many existing algorithms, such as branch and bound algorithm [51], may not apply to a large-scale problem since the time complexity exponentially increases with the number of the integer variables, particularly with the multi-dimension resource allocation variables  $\{x_{ik}, y_{kn}, b, T_1\}$ . Instead of looking for search methods, in what follows, we discuss the more efficient solution approaches for the micro-batching problem and the MSP problem, respectively.



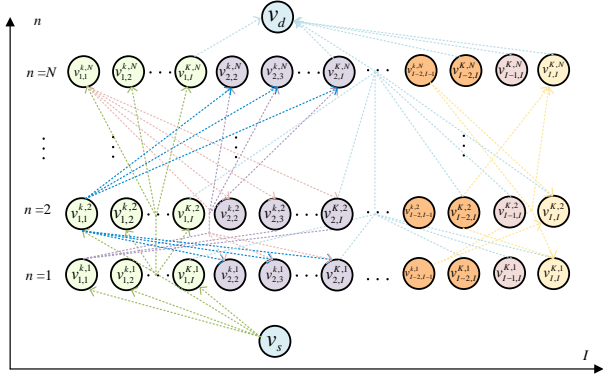


Fig. 3: The graph representation of the MSP problem.

### C. Solution to the Micro-batching Problem

By fixing the decision variables  $x_{ik}$ ,  $y_{kn}$  and  $T_1$  in  $\mathcal{P}2$ , the micro-batching problem can be expressed as

$$\begin{aligned} \mathcal{P}3 : \min_{\{b\}} & T_f(b) + \xi(b) \cdot T_1 \\ \text{s.t.} & \text{C3, C7 - C16,} \end{aligned} \quad (17)$$

Thus, the subproblem  $\mathcal{P}3$  is an integer linear programming (ILP) problem. We have the following theorem.

**Theorem 1.** For Problem  $\mathcal{P}3$ , the optimal micro-batch size  $b^*$  is given by

$$b^* = \begin{cases} b_1^*, & 0 < b \leq \min\{b_{th}^c, b_{th}^s\}, \\ b_2^*, & 0 < \max\{b_{th}^c, b_{th}^s\} \leq b, \\ b_3^*, & 0 < b_{th}^c < b < b_{th}^s, \\ b_4^*, & 0 < b_{th}^s < b < b_{th}^c, \end{cases} \quad (18)$$

Moreover,  $b_1^*$ ,  $b_2^*$ ,  $b_3^*$  and  $b_4^*$  are derived in (27), (32), (36) and (40), respectively.

*Proof.* Please see Appendix A.  $\square$

### D. Solution to the MSP Problem

By fixing the micro-batch  $b$ , the MSP problem can be formulated as

$$\begin{aligned} \mathcal{P}4 : \min_{\{x, y, T_1\}} & T_f(x, y) + \xi \cdot T_1 \\ \text{s.t.} & \text{C1, C2, C4 - C16,} \end{aligned} \quad (19)$$

which is a Mixed Integer Nonlinear Programming (MINLP) problem. Fortunately, we find that it falls into a combinatorial optimization problem (COP) with a combined min-max and min-sum objective function [52]. To tackle this problem, we convert the search space for the split and placement decisions into an undirected graph  $G = (\mathbf{V}, \mathbf{E})$ , where the set of vertices can be expressed by

$$\mathbf{V} = \{v_{(i-m),i}^{k,n} \mid \forall k \in [1, K], n \in \mathcal{N}, i \in [1, I], m \in [0, i-1]\}, \quad (20)$$

where a single vertex  $v_{(i-m),i}^{k,n}$  represents the decision of allocating the  $(i-m)$ -th layer to the  $i$ -th layer to the  $k$ -th submodel on the  $n$ -th edge node with all clients grouped into

one virtual node for  $k = 1$  and servers for  $k \in [2, K]$ . Here,  $m \in [0, i-1]$ . Besides, the set of vertices  $\mathbf{V}$  comprise all possible assignment decisions. Then, we can easily connect the vertex following Constraints C1, C2 and C4-C16

$$\begin{aligned} \mathbf{E} = \{ & (v_{(i-m),i}^{k,n}, v_{(i+1),(i+1+m')}^{(k+1),n'}) \mid \forall k \in [1, K-1], \\ & n, n' \in \mathcal{N}, n \neq n', i \in [1, I], \\ & m \in [0, i-1], m' \in [0, I-i-1]\}, \end{aligned} \quad (21)$$

where an edge  $(v_{(i-m),i}^{k,n}, v_{(i+1),(i+1+m')}^{(k+1),n'})$  represents choosing assignment  $v_{(i+1),(i+1+m')}^{(k+1),n'}$  after assignment  $v_{(i-m),i}^{k,n}$ . We set the weight of the edge to be the sum of latency of transferring data between the submodel  $k$  and  $(k+1)$  and the computing latency on client/server  $n$ , which can be expressed as

$$c(v_{(i-m),i}^{k,n}, v_{(i+1),(i+1+m')}^{(k+1),n'}) = \begin{cases} \max_{n \in \mathcal{N}_c} \{t_{1,n}^F(b, \mathbf{x}) + \sum_{n'=1}^N y_{2n'} t_{1,nn'}^F(\mathbf{x}, b)\} + \max_{n \in \mathcal{N}_c} \{ \\ t_{1,n}^B(b, \mathbf{x}) + \sum_{n'=1}^N y_{2n'} t_{1,nn'}^B(\mathbf{x}, b)\}, & k = 1, \\ t_{k,nn'}^F(\mathbf{x}, b) + t_{k,nn'}^B(\mathbf{x}, b) + t_{k,n}^F(b, \mathbf{x}) + t_{k,n}^B(b, \mathbf{x}), & \forall k \in [2, K-1], \end{cases} \quad (22)$$

where computing latency is set to be the maximum computing latency of all clients if  $k = 1$ . Furthermore, we add the virtual source vertex  $v_s$  and destination vertex  $v_d$ , respectively, where the weights of edges between  $v_s$  or  $v_d$  and any edge node in the graph are set to zero, i.e.,  $c(v_s, v_{1,(1+m')}^{1,n'}) = 0$  and  $c(v_{(I-m),I}^{K,n}, v_d) = 0$ .

To solve the MSP problem with the combined min-max and min-sum objective, we propose an efficient algorithm to find the optimal solution via the defined graph. Then, we sort the cost of edges in descending order to construct subgraphs. Given an edge  $e \in \mathbf{E}$ , we generate a subgraph that each path from the source vertex to the destination vertex in the subgraph should contain  $e$ . The process is repeated until we go through all the edges. With each subgraph, we first use reformulation-linearization technique to handle the original min-sum part in Problem  $\mathcal{P}4$  which will be elaborated upon in Appendix B and calculate a lower bound for the objective to decide whether to search the subgraph or discard the graph. Once searching, the original MSP problem in  $\mathcal{P}4$  becomes finding the shortest path from  $v_s$  to  $v_d$ , and the vertices along this path form the layer splitting and model placement decisions  $\{x_{ik}, y_{kn}\}$ , i.e.,  $x_{ik} = 1$  and  $y_{kn} = 1$  if and only if  $v_{(i-m),i}^{k,n}$  is on the path. By transforming the COP Problem  $\mathcal{P}4$  into a graph, the heap-optimized Dijkstra's algorithm [53] is used to find the shortest path within each generated subgraph. The minimum bound of the total latency can be found by comparing the min-sum-min-max objectives by assuming  $e$  is the bottleneck link across all the subgraphs. For this reason, we call the process as bottleneck-aware shortest path algorithm, and the detailed procedure is summarized in **Algorithm 1**. We have the following results.

**Finding lower bounds and pruning:** To efficiently reduce the search space of bottleneck-aware shortest path algo-

**Algorithm 1:** Bottleneck-aware Shortest Path Algorithm for the MSP Problem.

---

**Input:** Graph  $G = (V, E)$ , the maximum GPU memory of the client or server  $M_n$ , the number of edge servers  $N$ , the neural network to be processed, micro-batch size  $b$ , mini-batch size  $B$ , channel-related parameters  $W_{nn'}$ ,  $N_0$ ,  $r_{nn'}$  and  $\gamma$ , server-related parameters  $p_n$ ,  $t_0^s$ ,  $t_0^c$ ,  $t_1^s$ ,  $t_1^c$ ,  $f_n$ ,  $\kappa_n$ ,  $L_t^* = +\infty$ .

**Output:** The optimal training latency  $L_t(x, y, T_1)$  per round, splitting decisions  $\{x_{ik}^* | i \in [1, I], k \in [1, K]\}$ , and placement decisions  $\{y_{kn}^* | k \in [1, K], n \in [1, N]\}$ .

- 1 Calculate the weights  $c(v_{(i-m),i}^{k,n}, v_{(i+1),i+1+m'}^{(k+1),n'})$  of all edges;
- 2 Sort edges  $e$  in descending order of their weight  $w(e)$ , resulting in set  $\mathbf{E}_w$ ;
- 3 Find the lower bound  $l_b$  for the original graph with LP solver by reformulating and linearizing the min-sum part in Problem  $\mathcal{P}_4$ ;
- 4 **for**  $e \in \mathbf{E}_w$  **do**
- 5     Generates a subgraph from  $G$  containing edge  $e$  where the cost of  $e$  is the maximum one in the subgraph;
- 6     **if**  $l_b + \xi \cdot w(e) > L_t^*$  **then**
- 7         Continue;
- 8     **end**
- 9     Find an optimal path in the subgraph that includes edge  $e$  using the heap-optimized Dijkstra's algorithm satisfying the min-sum function  $\varpi_h = \min T_f(\mathbf{x}, \mathbf{y})$  and the memory constraint;
- 10    Compute the min-sum-min-max objective  $L_t^h = \varpi_h + \xi \cdot w(e)$ ;
- 11    **if**  $L_t^h < L_t^*$  **then**
- 12        Update the training latency  $L_t^* \leftarrow L_t^h$ ;
- 13         $x_{ik}^* \leftarrow x_{ik}$  and  $y_{kn}^* \leftarrow y_{kn}$ ;
- 14    **end**
- 15    Exclude  $e$  from Graph  $G$ ;
- 16 **end**

---

rithm for the MSP problem, we introduce the reformulation-linearization approach [54] to compute a lower bound for the objective (see Appendix B). Specifically, the bound is achieved by relaxing quadratic constraints of the original problem. The relaxed problem is then solved as an linear programming (LP) problem using LP solver Gurobi [55], which computes the lower bound for min-sum function in the MSP problem. When repeating searching subgraphs, if the lower bound of min-sum part plus the cost of current edge exceeds the current best solution  $L_t^*$ , the subsequent subgraphs can be safely excluded from further exploration. In other words, subproblems that cannot achieve a better solution than the current best solution  $L_t^*$  can be terminated early, saving computation time (see **Algorithm 1**).

**Theorem 2.** *Algorithm 1 can obtain the optimal solution to*

**Algorithm 2:** BCD-based Splitting, Placement, and Micro-batching Algorithm.

---

**Input:** Convergence tolerance  $\vartheta$ , iteration index  $\tau = 0$ , maximum GPU memory of the  $n$ -th server  $M_n^s$ .

**Output:**  $b^*$ ,  $\mathbf{X}^*$ ,  $\mathbf{Y}^*$ .

- 1 Initialization:  $b^0$ ;
- 2 **while**  $|L_t(x_{ik}^\tau, y_{kn}^\tau, b^\tau) - L_t(x_{ik}^{\tau-1}, y_{kn}^{\tau-1}, b^{\tau-1})| \geq \vartheta$
- 3     **do**
- 4        $\tau \leftarrow \tau + 1$ ;
- 5       Obtain  $x_{ik}^\tau$ ,  $y_{kn}^\tau$  and  $T_1^\tau$  by **Algorithm 1** with fixed decision variables  $b^{\tau-1}$ ;
- 6       Obtain  $b^\tau$  based on (18) with fixed decision variables  $x_{ik}^\tau$ ,  $y_{kn}^\tau$  and  $T_1^\tau$ ;
- 7        $b^* = b^\tau$ ,  $\mathbf{X}^* = \{x_{ik}^\tau\}$ , and  $\mathbf{Y}^* = \{y_{kn}^\tau\}$ .
- 8     **end**

---

the MSP subproblem  $\mathcal{P}_4$ .

*Proof.* The MSP Problem  $\mathcal{P}_4$  is a min-sum-min-max problem, which can be optimally solved by our bottleneck-aware shortest path algorithm. The proof is omitted due to page limitation, and a similar proof can be found in [52].  $\square$

**Theorem 3.** *Algorithm 1 has the computational complexity is  $O(E \log E + E(V + E) \log V) = O(E(V + E) \log V)$ .*

*Proof.* We sort the edges of a graph according to their respective costs with the complexity of  $O(E \log E)$ . By checking every edge to generate a subgraph containing the current edge, the complexity is  $O(E)$ . Then, the total complexity of subgraph generation is  $O(E \log E)$ . Running the heap-optimized Dijkstra's algorithm on each subgraph has a complexity of  $O((V' + E') \log V' + (V'' + E'') \log V'')$ , where  $V'$  and  $E'$  are the number of vertices and edges in the subgraph before edge  $e$ , and  $V''$  and  $E''$  are the number of vertices and edges in the subgraph after edge  $e$ . In the worst case, the subgraph size is similar to the original graph, which can be approximated as  $O((V + E) \log V)$ . Thus, the total complexity of the approach is  $O(E \log E + E(V + E) \log V) = O(E(V + E) \log V)$ .  $\square$

### E. Splitting, Placement, and Micro-batching Design

As mentioned, we decompose the original MINLP Problem  $\mathcal{P}_2$  into an MSP subproblem and a micro-batching subproblem (i.e.,  $\mathcal{P}_3$  and  $\mathcal{P}_4$ ), and find the optimal solution to each subproblem. Then, we further propose a block-coordinate descent (BCD)-based algorithm [56] to solve the original Problem  $\mathcal{P}_2$ , which is detailed in **Algorithm 2**, where  $x_{ik}^\tau$ ,  $y_{kn}^\tau$ ,  $T_1^\tau$  and  $b^\tau$  represent  $x_{ik}$ ,  $y_{kn}$ ,  $T_1$ , and  $b$  at the  $\tau$ -th iteration. Despite the mixed-integer nature [57] of the original Problem  $\mathcal{P}_2$ , the BCD-based algorithm converges within only a few iterations. Note that by optimally solving the original variables in each iteration, the convergence of the BCD procedure can be guaranteed because it finds the optimal solution at each step. Our simulations in Section VI will further demonstrate that the proposed algorithm can achieve the near-optimal solution to the joint optimization problem.



TABLE II: Simulation Parameters.

Parameter	Value	Parameter	Value
$f_n$	1 ~ 10 TFLOPS	$I$	16
$B$	512	$M_n$	2 ~ 16 GB
$W_{nn'}$	10 ~ 200 MHz	$\vartheta$	0.01
$N_0$	-174 dBm/Hz	$b^0$	20
$\kappa_n$	$\frac{1}{32}$ FLOPs/byte	$N$	2 ~ 10
$d_{nn'}$	1 ~ 500 m	$t_0^c/t_0^s$	0.001 s
$\gamma$	3.5	$t_1^c/t_1^s$	0.001 s
$p_n$	100 ~ 500 mW	$[b_{th}^c, b_{th}^s]$	[32, 32]

## VI. SIMULATIONS

### A. Simulation Setup

In our simulations,  $N$  edge servers are deployed within a square area of  $0.5 \text{ km} \times 0.5 \text{ km}$  where the distance between any two servers is within 500 m. By default,  $N$  is set to 6. The computing capability  $f_n$  is distributed within [1, 10] TFLOPS [58]. We consider two cases of 5G Integrated Access Backhaul (IAB) scenarios to evaluate high-speed and low-speed communication networks. For the low-speed case, we consider 5G sub-6GHz by setting the available bandwidth per link from 10 MHz to 50 MHz for access and backhaul links; For high-speed case, we consider 5G mmWave with available bandwidth per link ranging from 100 MHz to 200 MHz. Besides, the noise spectral density of servers is set to -174 dBm/Hz [59]. Moreover, we consider the signal power  $p_n$  from 100 to 500 mW, and the computing intensity  $\kappa_n = 1/32$  FLOPs/byte. The path loss exponent is set to 3.5 according to the channel model in [60]. For readers' convenience, the detailed simulation parameters are summarized in Table II. We adopt the image classification datasets MNIST and CIFAR-10 [61] to evaluate the performance of the proposed pipelined SL for the model VGG-16 [22] under both IID and non-IID settings. Moreover, the mini-batch size  $B$  is set to 512, with the initial micro batch  $b$  set to 20 and  $[b_{th}^c, b_{th}^s]$  set to [32, 32]. Accordingly, based on the experiments in [47],  $t_0^c$ ,  $t_0^s$ ,  $t_1^c$  and  $t_1^s$  are set to 0.001 s to match  $b_{th}^c$  and  $b_{th}^s$ . The algorithms have been implemented on a computer equipped with an AMD Ryzen Threadripper PRO 5975WX and NVIDIA GeForce RTX 4090.

To demonstrate the advantages of our framework, we compare it with three benchmarks: 1) “Random Cut and Optimal Placement” (**RC + OP**) randomly partition the model into several submodels while adopting the proposed placement strategy. 2) “Random Placement and Optimal Cut” (**RP + OC**) employs the proposed model splitting strategy while randomly placing the submodels among edge servers. 3) **No Pipeline** employs our algorithm to optimize both model splitting and placement without dividing a mini-batch into multiple micro-batches for pipelining. Due to the optimality, “No Pipeline” also serves as the performance upper bound of directly applying the existing split inference/learning scheme without pipeline parallelism [29]. In many experiments, we defined total latency as the time required for the model to reach 75% test accuracy on CIFAR-10 under IID setting.

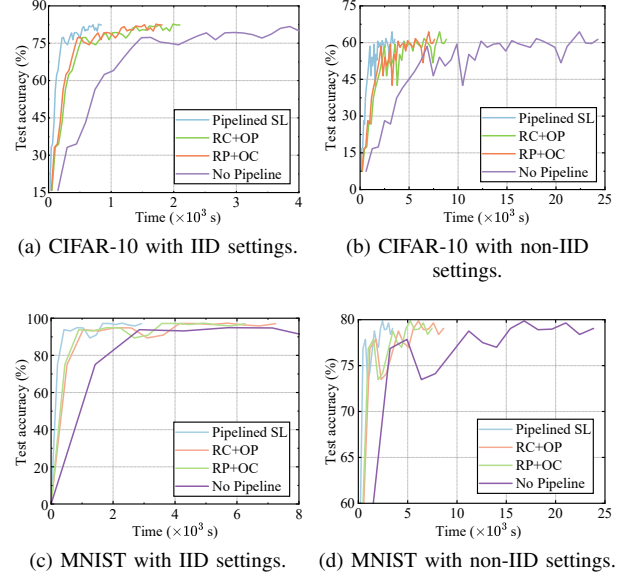


Fig. 4: The test accuracy of different SL schemes on CIFAR-10 and MNIST datasets using VGG-16.

### B. Performance Evaluation of the Proposed Pipelined SL Framework

Fig. 4 evaluates the test accuracy of our proposed pipelined SL scheme and other benchmarks across CIFAR-10 and MNIST datasets under both IID and non-IID settings. As observed, our scheme outperforms other benchmarks, including “RC + OP” and “RP + OC” schemes, demonstrating that both splitting and placement play a crucial role in enhancing training efficiency. More importantly, all the schemes substantially outperform the “No Pipeline” scheme since the “No Pipeline” approach requires almost  $3\times$  to  $7\times$  training time to reach the same accuracy level compared with other schemes. This underscores the effectiveness of pipelining in SL for multi-hop edge networks. By enabling parallel processing across multiple edge nodes, pipelined SL efficiently utilizes available resources, leading to faster model convergence without sacrificing accuracy.

Notice that different schemes indeed have the same converged accuracy because these schemes are essentially equivalent to centralized training, except that their total latency is different. In Fig. 5, we vary the networking settings to illustrate the total latency among the aforementioned schemes. As shown in Fig. 5(a), when we vary the number of servers from 2 to 10, the total latency for all schemes decreases significantly. This reduction is due to increased parallelism and more efficient model splitting and placement across more servers. The edge network benefits from enhanced flexibility, allowing for better utilization of computational resources. In Fig. 5(b), we observe the impact of bandwidth on total latency ranging from 10 MHz to 200 MHz. The total latency of all schemes decreases as bandwidth increases. This demonstrates that higher communication bandwidth reduces data transmission time between edge servers, which is crucial for SL where frequent inter-server communication occurs. Fig. 5(c)

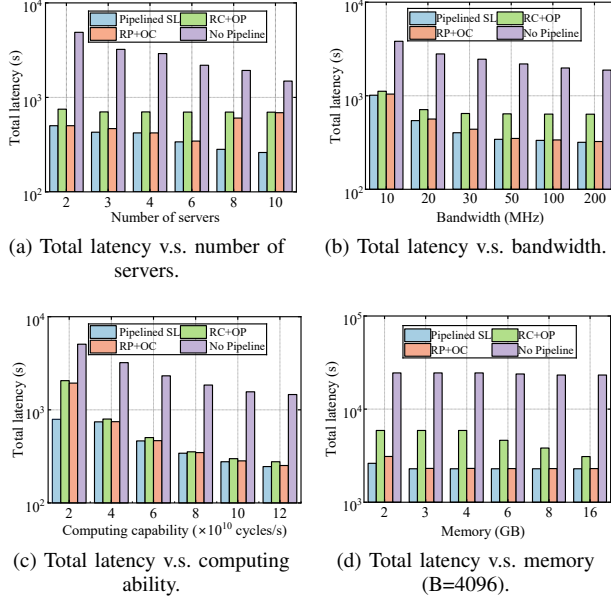


Fig. 5: The total latency versus varied network settings.

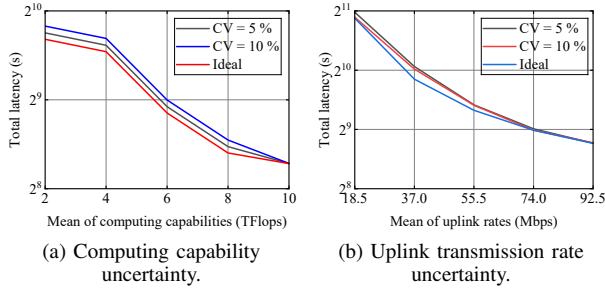


Fig. 6: The impact of network resource fluctuation on total latency on CIFAR-10 under IID setting using VGG-16.

illustrates the impact of computing capabilities on latency by varying computing capability from  $2 \times 10^{10}$  to  $12 \times 10^{10}$  cycles/s. It is unsurprising to see that enhanced computing power at edge servers shortens the local processing time required for training. Finally, Fig. 5(d) shows the effect of memory capacity on total latency by varying it from 2 GB to 16 GB. The latency for all schemes decreases with increased memory capacity, because larger memory space allows each server to handle more layers or larger micro-batches, adding flexibility in model splitting and placement.

In edge networks, computing and communication resources often fluctuate during training, resulting in discrepancies between the measured conditions (used for optimization) and the actual network conditions. To assess the impact of these measurement errors, we model the fluctuations in data rates and computing capabilities by introducing Gaussian noise with varying coefficients of variation (CV) [62], [63]. As illustrated in Fig. 6, our scheme maintains robustness across different levels of variation, resulting in only minor changes in overall latency. These results validate the effectiveness of our pipelined SL approach in fluctuating edge environments.

In Fig. 7, we evaluate the performance of our proposed

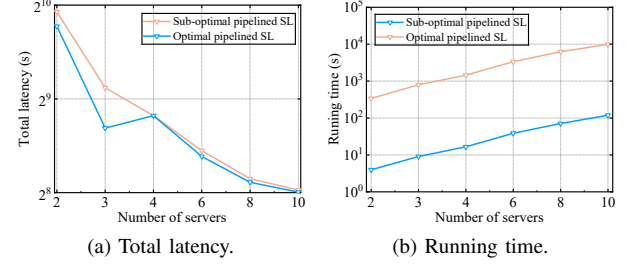


Fig. 7: The performance comparison of the sub-optimal and optimal pipelined SL.

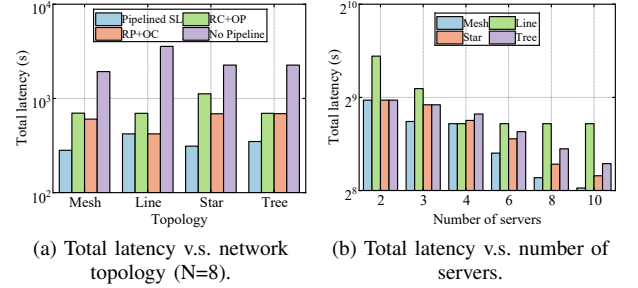


Fig. 8: Performance evaluation of the proposed pipelined SL framework across varied network topology.

suboptimal BCD algorithm and the optimal scheme, where the optimal scheme performs an exhaustive search on every possible micro-batch size, based on which we run Algorithm 1 to find the MSP solutions for each micro-batch size. Specifically, in Fig. 7(a), we observe that the total latency of our suboptimal solution closely matches that of the optimal scheme. For instance, with 10 servers, the optimal scheme achieves a total latency of approximately  $2.569 \times 10^2$  seconds, while the suboptimal BCD algorithm attains approximately  $2.609 \times 10^2$  seconds. This confirms that suboptimal BCD algorithm effectively provides near-optimal performance. Furthermore, Fig. 7(b) shows that as the number of servers increases from 2 to 10, the running time of the optimal scheme escalates drastically, reaching up to  $9.884 \times 10^3$  seconds (over 2.745 hours) at 10 servers. In contrast, the suboptimal BCD algorithm has a maximum running time of 119.132 seconds, demonstrating its scalability and efficiency. In practice, the running time is feasible even for the 10-server scenario since we consider a stationary edge network and the total training time can be for hours. In summary, our proposed algorithm achieves a suboptimal solution close to the optimal one while taking much less time to find the solution.

In Fig. 8, to validate the effectiveness of our solution to the MSP problem and the micro-batching problem across different physical network topologies, we compare the total latency for varied network topologies, including mesh, line, star, and tree structures. Specifically, Fig. 8(a) illustrates the relationship between total latency and varied network topologies. Mesh topology shows low latency due to high connectivity, while line topology has higher latency because of sequential connections. In the star topology, the central node needs to forward

messages between peripheral nodes, resulting in increased total latency due to the forwarding overhead at the central node. Tree topologies exhibit higher total latencies, attributed to their hierarchical communication constraints. In Fig. 8(b), We notice when  $N = 2$ , the mesh, star, and tree topologies exhibit identical total latency, while the unidirectional line topology experiences the longest total latency. Moreover, when we vary the number of servers from 2 to 10, the total latency for all network topologies decreases significantly. This reduction is due to increased parallelism and more efficient model splitting and placement across more servers.

## VII. CONCLUSION

In this paper, we addressed the joint optimization problem of model splitting and placement (MSP) and micro-batching for pipelined split learning (SL) in multi-hop edge networks under resource constraints. By taking pipeline parallelism into account, we discovered that the resulting MSP problem has a combined min-max and min-sum objective. Based on graph theory, we devise a bottleneck-aware shortest-path algorithm to solve the MSP problem optimally. Moreover, with fixed MSP outcomes, we also obtain the optimal micro-batch size for pipelined SL under communication-computing resource constraints. To minimize end-to-end training latency, we introduce an iterative algorithm that effectively solves the joint optimization problem. Our simulation findings consistently demonstrate the superior performance of our proposed approach compared with SL without pipeline parallelism.

## APPENDIX A PROOF OF THEOREM 1

To optimize the micro-batching subproblem  $\mathcal{P3}$  defined in (17), we consider the piecewise nature of the function induced by  $b_{th}^s$  and  $b_{th}^c$  and analyze each case separately. First, we arrange  $\lfloor \frac{b}{M} \rfloor$  data samples to each of the first  $M - 1$  clients and allocate the remaining  $b - (M - 1) \lfloor \frac{b}{M} \rfloor$  data samples to the  $M$ -th client. Thus, we have several situations:

(1) When  $0 < b \leq \min\{b_{th}^c, b_{th}^s\}$ , the optimization Problem  $\mathcal{P3}$  can be reformulated by

$$\mathcal{P3}' : \min_b T_f(b) + \xi(b) \cdot T_1$$

$$\text{s.t. } C3' : b \in \{1, 2, \dots, B\},$$

$$C7' : 0 \leq b_m \sum_{i=1}^I x_{i1}(\tilde{\varphi}_i + \tilde{\phi}_i + \tilde{\sigma}_i + \beta_i) \leq M_n, \quad \forall n \in \mathcal{N}_c,$$

$$C8' : 0 \leq b \sum_{i=1}^I (\tilde{\varphi}_i + \tilde{\phi}_i + \tilde{\sigma}_i + \beta_i) \left\{ x_{i1} + \sum_{k=2}^K y_{kn} \cdot (x_{ik} - x_{i(k-1)}) \right\} \leq M_n, \quad \forall n \in \mathcal{N} \setminus \mathcal{N}_c,$$

$$C9' : b \leq \frac{f_n \{T_1 - \sum_{k=2}^K y_{kn} t_0^s\}}{\sum_{k=2}^K y_{kn} \kappa_n \delta_{kn}^F}, \quad \forall n \in \mathcal{N} \setminus \mathcal{N}_c,$$

$$C10' : b_m \leq \frac{f_n (T_1 - t_0^c)}{\kappa_n \delta_{1n}^F}, \quad \forall n \in \mathcal{N}_c,$$

$$C11' : b \sum_{k=2}^{K-1} y_{kn} y_{(k+1)n'} \sum_{i=1}^I x_{ik} \varphi_i / r_{nn'} \leq T_1, \quad \forall n, n' \in \mathcal{N} \setminus \mathcal{N}_c,$$

$$C12' : b_m \sum_{i=1}^I x_{1k} \varphi_i / r_{nn'} \leq T_1, \quad \forall n \in \mathcal{N}_c, n' \in \mathcal{N} \setminus \mathcal{N}_c,$$

$$C15' : b \sum_{k=2}^{K-1} y_{kn} y_{(k+1)n'} \sum_{i=1}^I x_{ik} \phi_{(i+1)} / r_{nn'} \leq T_1, \quad \forall n, n' \in \mathcal{N} \setminus \mathcal{N}_c,$$

$$C16' : b_m \sum_{i=1}^I x_{i1} \phi_{(i+1)} / r_{nn'} \leq T_1, \quad \forall n \in \mathcal{N}_c, n' \in \mathcal{N} \setminus \mathcal{N}_c. \quad (25)$$

Herein, we try to obtain the optimal solution to Problem  $\mathcal{P3}'$ . Since we fix the decision variables  $x_{ik}$ ,  $y_{kn}$ , and  $T_1$ , the objective function  $\mathcal{Z}_1$  is only related to the variable  $b$ , which is expressed in Eq. (23).

According to the shape of the objective function, we can find the optimal point  $b_1$  in the feasible region (if it exists), which is expressed in Eq. (27). Moreover, according to Constraints  $C3'$  and  $C7' - C12'$ , the boundary variable  $b_v$  is defined in Eq. (24). To further minimize the value of the objection function while remaining in the feasible domain, the optimal micro-batch size is

$$b_1^* = \begin{cases} 1, & b_1 \leq 1, \\ b_1, & 1 < b_1 \leq \min\{b_v, B\}, \\ \min\{b_v, B\}, & \min\{b_v, B\} < b_1, \end{cases} \quad (26)$$

$$\text{where } b_1 = \arg \min_{b \in \{\lfloor \tilde{b}_1 \rfloor, \lceil \tilde{b}_1 \rceil\}} T_f(b) + \xi(b) \cdot T_1,$$

$$\begin{aligned} \tilde{b}_1 = & \left( B \cdot T_1 \left( \sum_{k=2}^K \sum_{n=1}^N y_{kn} \kappa_n \delta_{kn}^F / f_n + \sum_{n=1}^N \sum_{n'=1}^N \sum_{i=1}^I \Lambda \right. \right. \\ & + \max_{n \in \mathcal{N}_c} \left\{ \frac{1}{M} \kappa_n \delta_{1n}^F / f_n + \sum_{n'=1}^N y_{2n'} \frac{1}{M} \cdot \sum_{i=1}^I x_{i1} \varphi_i / r_{nn'} \right\} + \\ & \left. \left. \max_{n \in \mathcal{N}_c} \left\{ \sum_{n'=1}^N y_{2n'} \frac{1}{M} \cdot \sum_{i=1}^I x_{i1} \phi_{(i+1)} / r_{nn'} \right\} \right)^{-1} \right)^{\frac{1}{2}}. \end{aligned} \quad (27)$$

and

$$\Lambda = \frac{\sum_{k=2}^{K-1} y_{kn} y_{(k+1)n'} x_{ik} \varphi_i + \sum_{k=2}^{K-1} y_{kn} y_{(k+1)n'} x_{ik} \phi_{(i+1)}}{r_{nn'}}. \quad (28)$$

(2) When  $0 < \max\{b_{th}^s, b_{th}^c\} \leq b$ , the optimization Problem  $\mathcal{P3}$  can be reformulated by

$$\mathcal{P3}'' : \min_b T_f(b) + \xi(b) \cdot T_1$$

$$\text{s.t. } C3', C7' - C12', C15' - C16',$$

$$C13' : b \leq \frac{f_n \{T_1 - \sum_{k=2}^K y_{kn} t_1^s\}}{\sum_{k=2}^K y_{kn} \kappa_n \delta_{kn}^B} + b_{th}^s, \quad \forall n \in \mathcal{N} \setminus \mathcal{N}_c,$$

$$\mathcal{Z}_1 = b \left\{ \sum_{k=2}^K \sum_{n=1}^N \frac{y_{kn} \kappa_n \delta_{kn}^F}{f_n} + \sum_{n=1}^N \sum_{n'=1}^N \sum_{i=1}^I \frac{\sum_{k=2}^{K-1} y_{kn} y_{(k+1)n'} x_{ik} \varphi_i + \sum_{k=2}^{K-1} y_{kn} y_{(k+1)n'} x_{ik} \phi_{(i+1)}}{W_{nn'} \cdot \log \left( 1 + p_n(d_{nn'})^{-\gamma} / N_0 \right)} \right\} + T_1 \left\lceil \frac{B-b}{b} \right\rceil + (K-1)(t_0^s + t_1^s) + \max_{n \in \mathcal{N}_c} \{ b_m \kappa_n \delta_{1n}^F / f_n + t_0^c + \sum_{n'=1}^N y_{2n'} b_m \sum_{i=1}^I x_{i1} \varphi_i / r_{nn'} \} + \max_{n \in \mathcal{N}_c} \{ t_1^c + \sum_{n'=1}^N y_{2n'} b_m \sum_{i=1}^I x_{i1} \phi_{(i+1)} / r_{nn'} \}. \quad (23)$$

$$b_v = \min \left\{ \min_{n \in \mathcal{N} \setminus \mathcal{N}_c} \left\{ \left\lceil \frac{M_n}{\{x_{i1} + \sum_{k=2}^K y_{kn} (x_{ik} - x_{i(k-1)})\} \sum_{i=1}^I (\tilde{\varphi}_i + \tilde{\phi}_i + \tilde{\sigma}_i + \beta_i)} \right\rceil, \left\lceil \frac{f_n \{T_1 - \sum_{k=2}^K y_{kn} t_0^s\}}{\sum_{k=2}^K y_{kn} \kappa_n \delta_{kn}^F} \right\rceil, \right. \right. \\ \left. \left. \left\lceil \frac{T_1 r_{nn'}}{\sum_{k=2}^{K-1} y_{kn} y_{(k+1)n'} \sum_{i=1}^I x_{ik} \varphi_i} \right\rceil, \left\lceil \frac{T_1 r_{nn'}}{\sum_{k=2}^{K-1} y_{kn} y_{(k+1)n'} \sum_{i=1}^I x_{ik} \phi_{(i+1)}} \right\rceil \right\}, \right. \\ \left. \min_{n \in \mathcal{N}_c} \left\{ \left\lceil \frac{M \cdot M_n}{\sum_{i=1}^I x_{i1} (\tilde{\varphi}_i + \tilde{\phi}_i + \tilde{\sigma}_i + \beta_i)} \right\rceil, \left\lceil \frac{M T_1 r_{nn'}}{\sum_{i=1}^I x_{i1} \varphi_i} \right\rceil, \left\lceil \frac{M T_1 r_{nn'}}{\sum_{i=1}^I x_{i1} \phi_{(i+1)}} \right\rceil, \left\lceil \frac{M f_n (T_1 - t_0^c)}{\kappa_n \delta_{1n}^F} \right\rceil \right\} \right\}. \quad (24)$$

$$\mathcal{Z}_2 = b \left\{ \sum_{k=2}^K \sum_{n=1}^N \frac{y_{kn} \kappa_n (\delta_{kn}^F + \delta_{kn}^B)}{f_n} + \sum_{n=1}^N \sum_{n'=1}^N \sum_{i=1}^I \frac{\sum_{k=2}^{K-1} y_{kn} y_{(k+1)n'} x_{ik} \varphi_i + \sum_{k=2}^{K-1} y_{kn} y_{(k+1)n'} x_{ik} \phi_{(i+1)}}{W_{nn'} \cdot \log \left( 1 + p_n(d_{nn'})^{-\gamma} / N_0 \right)} \right\} + T_1 \left\lceil \frac{B-b}{b} \right\rceil - \\ (K-1) \left\{ \frac{\kappa_n \delta_{kn}^B b_{th}^s}{f_n^s} - (t_0^s + t_1^s) \right\} + \max_{n \in \mathcal{N}_c} \{ b_m \frac{\kappa_n \delta_{1n}^F}{f_n} + t_0^c + \sum_{n'=1}^N y_{2n'} b_m \sum_{i=1}^I \frac{x_{i1} \varphi_i}{r_{nn'}} \} \\ + \max_{n \in \mathcal{N}_c} \{ (b_m - b_{th}^c) \frac{\kappa_n \delta_{1n}^B}{f_n} + t_1^c + \sum_{n'=1}^N y_{2n'} b_m \sum_{i=1}^I \frac{x_{i1} \phi_{(i+1)}}{r_{nn'}} \}. \quad (29)$$

$$C14' : b \leq \frac{M f_n (T_1 - t_1^c)}{\kappa_n \delta_{1n}^B} + M b_{th}^c, \forall n \in \mathcal{N}_c. \quad (30)$$

Similarly, to minimize the value of the objection function  $\mathcal{Z}_2$  in Eq. (29), the following variable  $b_2^*$  is set to:

$$b_2^* = \begin{cases} 1, & b_2 \leq 1, \\ b_2, & 1 < b_2 \leq \min \{b_v', B\}, \\ \min \{b_v', B\}, & \min \{b_v', B\} < b_2, \end{cases} \quad (31)$$

where  $b_2 = \arg \min_{b \in \{\lfloor \tilde{b}_2 \rfloor, \lceil \tilde{b}_2 \rceil\}} T_f(b) + \xi(b) \cdot T_1$ . Herein,  $\tilde{b}_2$  and  $b_v'$  can be denoted by

$$\tilde{b}_2 = \left\lceil \left( B \cdot T_1 \left( \sum_{k=2}^K \sum_{n=1}^N \frac{y_{kn} \kappa_n (\delta_{kn}^F + \delta_{kn}^B)}{f_n} + \sum_{n=1}^N \sum_{n'=1}^N \sum_{i=1}^I \Lambda \right. \right. \right. \\ \left. \left. + \max_{n \in \mathcal{N}_c} \left\{ \frac{1}{M} \kappa_n \frac{\delta_{1n}^F}{f_n} + \sum_{n'=1}^N y_{2n'} \frac{1}{M} \cdot \sum_{i=1}^I \frac{x_{i1} \varphi_i}{r_{nn'}} \right\} + \max_{n \in \mathcal{N}_c} \left\{ \frac{1}{M} \right. \right. \right. \\ \left. \left. \left. \kappa_n \delta_{1n}^B / f_n + \sum_{n'=1}^N y_{2n'} \frac{1}{M} \cdot \sum_{i=1}^I x_{i1} \phi_{(i+1)} / r_{nn'} \right\} \right)^{-1} \right\rceil^{\frac{1}{2}}. \quad (32)$$

$$b_v' = \min \left\{ b_v, \min_{n \in \mathcal{N} \setminus \mathcal{N}_c} \left\{ \left\lceil \frac{f_n \{T_1 - \sum_{k=2}^K y_{kn} t_0^s\}}{\sum_{k=2}^K y_{kn} \kappa_n \delta_{kn}^B} + b_{th}^s \right\rceil, \right. \right. \\ \left. \left. \min_{n \in \mathcal{N}_c} \left\{ \left\lceil \frac{M f_n (T_1 - t_1^c)}{\kappa_n \delta_{1n}^B} + M b_{th}^c \right\rceil \right\} \right\} \right\}. \quad (33)$$

(3) Similarly, when  $0 < b_{th}^c < b < b_{th}^s$ , the optimization Problem  $\mathcal{P}3$  can be reformulated by

$$\mathcal{P}3''' : \min_b T_f(b) + \xi(b) \cdot T_1 \\ \text{s.t. } C3', C7' - C12', C15' - C16', \\ C14' : b \leq \frac{M f_n (T_1 - t_1^c)}{\kappa_n \delta_{1n}^B} + M b_{th}^c, \forall n \in \mathcal{N}_c, \quad (34)$$

To minimize the value of the objection function, the following variable  $b_3^*$  is set to

$$b_3^* = \begin{cases} 1, & b_3 \leq 1, \\ b_3, & 1 < b_3 \leq \min \{b_v'', B\}, \\ \min \{b_v'', B\}, & \min \{b_v'', B\} < b_3, \end{cases} \quad (35)$$

where  $b_3 = \arg \min_{b \in \{\lfloor \tilde{b}_3 \rfloor, \lceil \tilde{b}_3 \rceil\}} T_f(b) + \xi(b) \cdot T_1$ , and  $\tilde{b}_3$  can be

expressed by

$$\tilde{b}_3 = \left[ \left( B \cdot T_1 \left( \sum_{k=2}^K \sum_{n=1}^N \frac{y_{kn} \kappa_n \delta_{kn}^F}{f_n} + \sum_{n=1}^N \sum_{n'=1}^N \sum_{i=1}^I \Lambda + \max_{n \in \mathcal{N}_c} \left\{ \frac{1}{M} \frac{\kappa_n \delta_{1n}^F}{f_n} + \sum_{n'=1}^N y_{2n'} \frac{1}{M} \cdot \sum_{i=1}^I x_{i1} \varphi_i / r_{nn'} \right\} + \max_{n \in \mathcal{N}_c} \left\{ \frac{1}{M} \frac{\kappa_n \delta_{1n}^B}{f_n} + \sum_{n'=1}^N y_{2n'} \frac{1}{M} \cdot \sum_{i=1}^I x_{i1} \phi_{(i+1)} / r_{nn'} \right\} \right)^{\frac{1}{2}} \right], \quad (36)$$

and  $b_v''$  is denoted by

$$b_v'' = \min \left\{ b_v, \min_{n \in \mathcal{N}_c} \left\{ \left\lfloor \frac{n f_n (T_1 - t_1^c)}{\kappa_n \delta_{1n}^B} + M b_{th}^c \right\rfloor \right\} \right\}. \quad (37)$$

(4) Similarly, when  $0 < b_{th}^s < b < b_{th}^c$ , the optimization Problem  $\mathcal{P}3$  can be reformulated by

$$\begin{aligned} \mathcal{P}3''': \min_b & T_f(b) + \xi(b) \cdot T_1 \\ \text{s.t.} & \text{C3}', \text{C7}' - \text{C12}', \text{C15}' - \text{C16}', \\ & \text{C13}': b \leq \frac{f_n \{T_1 - \sum_{k=2}^K y_{kn} t_1^s\}}{\sum_{k=2}^K y_{kn} \kappa_n \delta_{kn}^B} + b_{th}^s, \quad \forall n \in \mathcal{N} \setminus \mathcal{N}_c. \end{aligned} \quad (38)$$

To minimize the value of the objection function, the following variable  $b_4^*$  is set to

$$b_4^* = \begin{cases} 1, & b_4 \leq 1, \\ b_4, & 1 < b_4 \leq \min \{b_v''', B\}, \\ \min \{b_v''', B\}, & \min \{b_v''', B\} < b_4, \end{cases} \quad (39)$$

where  $b_4 = \arg \min_{b \in \{[b_4], [\tilde{b}_4]\}} T_f(b) + \xi(b) \cdot T_1$  and  $\tilde{b}_4$  is defined by

$$\tilde{b}_4 = \left[ \left( B \cdot T_1 \left( \sum_{k=2}^K \sum_{n=1}^N \frac{y_{kn} \kappa_n (\delta_{kn}^F + \delta_{kn}^B)}{f_n} + \sum_{n=1}^N \sum_{n'=1}^N \sum_{i=1}^I \Lambda + \max_{n \in \mathcal{N}_c} \left\{ \frac{1}{M} \frac{\kappa_n \delta_{1n}^F}{f_n} + \sum_{n'=1}^N y_{2n'} \frac{1}{M} \sum_{i=1}^I \frac{x_{i1} \varphi_i}{r_{nn'}} \right\} + \max_{n \in \mathcal{N}_c} \left\{ \sum_{n'=1}^N y_{2n'} \frac{1}{M} \cdot \sum_{i=1}^I x_{i1} \phi_{(i+1)} / r_{nn'} \right\} \right)^{\frac{1}{2}} \right]. \quad (40)$$

and  $b_v'''$  is denoted by

$$b_v''' = \min \left\{ b_v, \min_{n \in \mathcal{N} \setminus \mathcal{N}_c} \left\{ \left\lfloor \frac{f_n \{T_1 - \sum_{k=2}^K y_{kn} t_0^s\}}{\sum_{k=2}^K y_{kn} \kappa_n \delta_{kn}^B} + b_{th}^s \right\rfloor \right\} \right\}. \quad (41)$$

Thus, the proof is completed.

## APPENDIX B

### REFORMULATION AND LINEARIZATION OF MSP PROBLEM

To compute a lower bound for the min-sum objective in Problem  $\mathcal{P}4$ , we need to reformulate and linearize the original problem. Above all, we define  $\boldsymbol{\mu} = \{\mu_{knik} | k \in [1, K-1], n \in \mathcal{N}\}$  and  $\boldsymbol{\zeta} = \{\zeta_{knik(k+1)n'i'(k+1)} | k \in [1, K-1], n, n' \in \mathcal{N}\}$ .

Moreover,  $\mu_{knik} \in [0, 1]$  and  $\zeta_{knik(k+1)n'i'(k+1)} \in [0, 1]$  are continuous variables and expressed by

$$\begin{aligned} \mu_{knik} &= y_{kn} \sum_{i=1}^I x_{ik}, \quad \mu_{kni(k-1)} = y_{kn} \sum_{i=1}^I x_{i(k-1)}, \\ \zeta_{knik(k+1)n'i'(k+1)} &= y_{kn} \sum_{i=1}^I x_{ik} \cdot y_{(k+1)n'} \sum_{i'=1}^I x_{i'(k+1)}. \end{aligned} \quad (42)$$

In this section, considering the piecewise nature of the function induced by  $b_{th}^s$  and  $b_{th}^c$  and analyze each case separately, we have following situations:

(1) When  $0 < b \leq \min\{b_{th}^c, b_{th}^s\}$ , the reformulation of min-sum part in  $\mathcal{P}4$  can be expressed by

$$\begin{aligned} \mathcal{P}4': \min_{\{\boldsymbol{\mu}, \boldsymbol{\zeta}\}} & T_f(\boldsymbol{\mu}, \boldsymbol{\zeta}) = b \max_{n \in \mathcal{N}_c} \left\{ \sum_{n'=1}^N \frac{\zeta_{1ni12n'i'2\phi(i+1)}}{M r_{nn'}} \right\} + \\ & A(\boldsymbol{\mu}, \boldsymbol{\zeta}) + b \left\{ \sum_{k=2}^K \sum_{n=1}^N \kappa_n ((\mu_{knik} - \mu_{kni(k-1)}) w_i) / f_n \right\}, \\ \text{s.t.} & \text{C5}^\dagger: \sum_{i=1}^{I'} \mu_{knik} \leq \sum_{i=1}^{I'} \mu_{kni(k-1)}, \quad \forall k \in [2, K-1], I' \in [1, I], \\ & \text{C6}^\dagger: \sum_{n=1}^N \mu_{knik} = 1, \quad \forall k \in [1, K], \\ & \text{C7}^\dagger: 0 \leq m_1(\mu_{1ni1}, b) \leq M_n, \quad \forall n \in \mathcal{N}_c, \\ & \text{C8}^\dagger: 0 \leq \sum_{k=2}^K b(\mu_{knik} - \mu_{kni(k-1)}) \cdot (\tilde{\varphi}_i + \tilde{\phi}_i + \tilde{\sigma}_i + \beta_i) \leq M_n, \quad \forall n \in \mathcal{N} \setminus \mathcal{N}_c, \\ & \text{C17}^\dagger: \sum_{k=1}^{K-1} \zeta_{knik(k+1)n'i'(k+1)} = \mu_{(k+1)n'i'(k+1)}, \quad \forall n, n' \in \mathcal{N}, \\ & \text{C18}^\dagger: \sum_{k=2}^K \zeta_{knik(k+1)n'i'(k+1)} = \mu_{knik}, \quad \forall n, n' \in \mathcal{N}. \end{aligned} \quad (43)$$

Moreover,  $A(\boldsymbol{\zeta})$  can be expressed by

$$\begin{aligned} A(\boldsymbol{\mu}, \boldsymbol{\zeta}) &= b \sum_{n=1}^N \sum_{n'=1}^N \sum_{k=2}^{K-1} \frac{\zeta_{knik(k+1)n'i'(k+1)} (\varphi_i + \phi_{(i+1)})}{r_{nn'}} + \\ & b \max_{n \in \mathcal{N}_c} \left\{ \frac{\kappa_n \mu_{1ni1} w_i}{M f_n} + \sum_{n'=1}^N \frac{\zeta_{1ni12n'i'2\varphi_i}}{M r_{nn'}} \right\} + K(t_0^S + t_1^S). \end{aligned} \quad (44)$$

(2) When  $0 < \max\{b_{th}^s, b_{th}^c\} \leq b$ , the optimization Problem  $\mathcal{P}4$  can be reformulated by

$$\begin{aligned} \mathcal{P}4'': \min_{\{\boldsymbol{\mu}, \boldsymbol{\zeta}\}} & T_f(\boldsymbol{\mu}, \boldsymbol{\zeta}) = b \left\{ \sum_{k=2}^K \sum_{n=1}^N \kappa_n ((\mu_{knik} - \mu_{kni(k-1)}) w_i \right. \\ & \left. + (\mu_{knik} - \mu_{kni(k-1)}) \rho_i) / f_n \right\} - (K-1) \left\{ \frac{\kappa_n \delta_{kn}^B b_{th}^s}{f_n} \right\} + \end{aligned}$$

$$b \max_{n \in \mathcal{N}_c} \left\{ \left( \frac{1}{M} - b_{th}^c \right) \frac{\kappa_n \mu_{1ni1} \rho_i}{f_n} + \sum_{n'=1}^N \frac{\zeta_{1ni12n'i'2} \phi_{(i+1)}}{Mr_{nn'}} \right\} \\ + A(\boldsymbol{\mu}, \boldsymbol{\zeta}), \\ \text{s.t. } C5^\dagger - C8^\dagger, C17^\dagger, C18^\dagger. \quad (45)$$

(3) Similarly, when  $0 < b_{th}^c < b < b_{th}^s$ , the optimization Problem  $\mathcal{P}4$  can be reformulated by

$$\mathcal{P}4''' : \min_{\{\boldsymbol{\mu}, \boldsymbol{\zeta}\}} T_f(\boldsymbol{\mu}, \boldsymbol{\zeta}) = b \max_{n \in \mathcal{N}_c} \left\{ \sum_{n'=1}^N \frac{\zeta_{1ni12n'i'2} \phi_{(i+1)}}{Mr_{nn'}^c} \right\} \\ + A(\boldsymbol{\mu}, \boldsymbol{\zeta}) + b \left\{ \sum_{k=2}^K \sum_{n=1}^N \kappa_n ((\mu_{knik} - \mu_{kni(k-1)}) w_i + \right. \\ \left. (\mu_{knik} - \mu_{kni(k-1)}) \rho_i) / f_n \right\}, \\ \text{s.t. } C5^\dagger - C8^\dagger, C17^\dagger, C18^\dagger. \quad (46)$$

(4) Similarly, when  $0 < b_{th}^s < b < b_{th}^c$ , the optimization Problem  $\mathcal{P}4$  can be reformulated by

$$\mathcal{P}4'''' : \min_{\{\boldsymbol{\mu}, \boldsymbol{\zeta}\}} T_f(\boldsymbol{\mu}, \boldsymbol{\zeta}) = A(\boldsymbol{\mu}, \boldsymbol{\zeta}) - (K-1) \left\{ \frac{\kappa_n \delta_{kn}^B b_{th}^s}{f_n} \right\} + \\ + b \left\{ \sum_{k=2}^K \sum_{n=1}^N \kappa_n (\mu_{knik} - \mu_{kni(k-1)}) w_i / f_n \right\} + b \max_{n \in \mathcal{N}_c} \\ \left\{ \left( \frac{1}{M} - b_{th}^c \right) \frac{\kappa_n \mu_{1ni1} \rho_i}{f_n} + \sum_{n'=1}^N \frac{\zeta_{1ni12n'i'2} \phi_{(i+1)}}{Mr_{nn'}} \right\}, \\ \text{s.t. } C5^\dagger - C8^\dagger, C17^\dagger, C18^\dagger. \quad (47)$$

By reformulating and linearizing the original min-sum part, it proves that the optimized value of  $T_f(\boldsymbol{\mu}, \boldsymbol{\zeta})$  function does not exceed the optimal value of the original min-sum problem, thus providing a lower bound [54].

## REFERENCES

- [1] Y. Mao, C. You, J. Zhang, K. Huang, and K. B. Letaief, "A survey on mobile edge computing: The communication perspective," *IEEE Communications Surveys & Tutorials*, vol. 19, no. 4, pp. 2322–2358, Aug., 2017.
- [2] Z. Lin, W. Wei, Z. Chen, C.-T. Lam, X. Chen, Y. Gao, and J. Luo, "Hierarchical split federated learning: Convergence analysis and system optimization," *IEEE Transactions on Mobile Computing*, 2025.
- [3] M. Hu, J. Zhang, X. Wang, S. Liu, and Z. Lin, "Accelerating federated learning with model segmentation for edge networks," *IEEE Transactions on Green Communications and Networking*, 2024.
- [4] Z. Lin, X. Hu, Y. Zhang, Z. Chen, Z. Fang, X. Chen, A. Li, P. Vepakomma, and Y. Gao, "Splitlora: A split parameter-efficient fine-tuning framework for large language models," *arXiv preprint arXiv:2407.00952*, 2024.
- [5] Z. Wang, K. Huang, and Y. C. Eldar, "Spectrum breathing: Protecting over-the-air federated learning against interference," *IEEE Trans. Wireless Commun.*, vol. 23, no. 8, pp. 10058–10071, 2024.
- [6] Z. Ning, P. Dong, X. Wang, X. Hu, L. Guo, B. Hu, Y. Guo, T. Qiu, and R. Y. K. Kwok, "Mobile edge computing enabled 5G health monitoring for internet of medical things: A decentralized game theoretic approach," *IEEE Journal on Selected Areas in Communications*, vol. 39, no. 2, pp. 463–478, 2021.
- [7] N. Mehandru, B. Y. Miao, E. R. Almaraz, M. Sushil, A. J. Butte, and A. Alaa, "Evaluating large language models as agents in the clinic," *NPJ digital medicine*, vol. 7, no. 1, p. 84, 2024.
- [8] Y. Tang, Z. Chen, A. Li, T. Zheng, Z. Lin, J. Xu, P. Lv, Z. Sun, and Y. Gao, "Merit: Multimodal wearable vital sign waveform monitoring," *arXiv preprint arXiv:2410.00392*, 2024.
- [9] T. Qiu, J. Chi, X. Zhou, Z. Ning, M. Atiquzzaman, and D. O. Wu, "Edge computing in industrial internet of things: Architecture, advances and challenges," *IEEE Communications Surveys & Tutorials*, vol. 22, no. 4, pp. 2462–2488, 2020.
- [10] Z. Wang, A. E. Kalør, Y. Zhou, P. Popovski, and K. Huang, "Ultra-low-latency edge inference for distributed sensing," 2024. [Online]. Available: <https://arxiv.org/abs/2407.13360>
- [11] T. Taleb, S. Dutta, A. Ksentini, M. Iqbal, and H. Flinck, "Mobile edge computing potential in making cities smarter," *IEEE Communications Magazine*, vol. 55, no. 3, pp. 38–43, 2017.
- [12] Z. Lin, Y. Zhang, Z. Chen, Z. Fang, C. Wu, X. Chen, Y. Gao, and J. Luo, "Leo-split: A semi-supervised split learning framework over leo satellite networks," *arXiv preprint arXiv:2501.01293*, 2025.
- [13] P. Voigt and A. Von dem Bussche, "The EU general data protection regulation (GDPR)," *A Practical Guide, 1st Ed., Cham: Springer International Publishing*, vol. 10, no. 3152676, pp. 10–5555, 2017.
- [14] Z. Lin, G. Qu, X. Chen, and K. Huang, "Split learning in 6g edge networks," *IEEE Wireless Communications*, 2024.
- [15] P. Zhang, G. Zeng, T. Wang, and W. Lu, "Tinyllama: An open-source small language model," *arXiv preprint arXiv:2401.02385*, 2024.
- [16] G. Qu, Q. Chen, W. Wei, Z. Lin, X. Chen, and K. Huang, "Mobile edge intelligence for large language models: A contemporary survey," *IEEE Communications Surveys & Tutorials*, pp. 1–1, 2025.
- [17] O. Gupta and R. Raskar, "Distributed learning of deep neural network over multiple agents," *Journal of Network and Computer Applications*, vol. 116, pp. 1–8, 2018.
- [18] P. Vepakomma, O. Gupta, T. Swedish, and R. Raskar, "Split Learning for Health: Distributed Deep Learning Without Sharing Raw Patient Data," *arXiv preprint arXiv:1812.00564*, Dec. 2018.
- [19] Y. J. Ha, M. Yoo, S. Park, S. Jung, and J. Kim, "Secure aerial surveillance using split learning," in *2021 Twelfth International Conference on Ubiquitous and Future Networks (ICUFN)*. IEEE, 2021, pp. 434–437.
- [20] Z. Lin, G. Qu, X. Chen, and K. Huang, "Split learning in 6G edge networks," *IEEE Wireless Communications*, vol. 31, no. 4, pp. 170–176, Aug., 2024.
- [21] HuaweiTech, "ITU-R WP5D completed the recommendation framework for IMT-2030 (global 6G vision)," 2023. [Online]. Available: <https://www.huawei.com/en/huaweitech/future-technologies/itu-r-wp5d-completed-recommendation-framework-imt-2030>
- [22] K. Simonyan and A. Zisserman, "Very deep convolutional networks for large-scale image recognition," *arXiv preprint arXiv:1409.1556*, 2014.
- [23] A. Krizhevsky, I. Sutskever, and G. E. Hinton, "Imagenet classification with deep convolutional neural networks," in *Advances in Neural Information Processing Systems*, vol. 25. Curran Associates, Inc., 2012, pp. 1097–1105.
- [24] A. R. Khousas, M. R. Bouadjenek, H. Hacid, and S. Aryal, "Training machine learning models at the edge: A survey," *arXiv preprint arXiv:2403.02619*, Mar., 2024.
- [25] Raspberry Pi Foundation, "Raspberry Pi 4 model B specifications," 2021. [Online]. Available: <https://www.raspberrypi.com/products/raspberry-pi-4-model-b/specifications/>
- [26] NVIDIA Corporation, "NVIDIA Tesla V100 GPU Architecture," 2017. [Online]. Available: <https://images.nvidia.com/content/volta-architecture/pdf/volta-architecture-whitepaper.pdf>
- [27] Y. Huang, Y. Cheng, A. Bapna, O. Firat, D. Chen, M. Chen, H. Lee, J. Ngiam, Q. V. Le, Y. Wu *et al.*, "GPipe: Efficient training of giant neural networks using pipeline parallelism," in *Proc. Adv. Neural Inform. Process. Syst. (NeurIPS)*, Vancouver, BC, Canada, Dec., 2019, pp. 103–112.
- [28] D. Narayanan, A. Harlap, A. Phanishayee, V. Seshadri, N. R. Devanur, G. R. Ganger, P. B. Gibbons, and M. Zaharia, "PipeDream: Generalized pipeline parallelism for DNN training," in *Proceedings of the ACM Symposium on Operating Systems Principles*, New York, NY, USA, Oct., 2019, p. 1–15.
- [29] S. Wang, X. Zhang, H. Uchiyama, and H. Matsuda, "Hivemind: Towards cellular native machine learning model splitting," *IEEE Journal on Selected Areas in Communications*, vol. 40, no. 2, pp. 626–640, Feb. 2022.
- [30] Z. Wang, Q. Zeng, H. Zheng, and K. Huang, "Revisiting outage for edge inference systems," 2025. [Online]. Available: <https://arxiv.org/abs/2504.03686>
- [31] Z. Liu, X. Chen, H. Wu, Z. Wang, X. Chen, D. Niyato, and K. Huang, "Integrated sensing and edge AI: Realizing intelligent perception in 6G," 2025. [Online]. Available: <https://arxiv.org/abs/2501.06726>
- [32] Y. Kang, J. Hauswald, C. Gao, A. Rovinski, T. Mudge, J. Mars, and L. Tang, "Neurosurgeon: Collaborative intelligence between the cloud and mobile edge," in *Proceedings of the Twenty-Second International*



- Conference on Architectural Support for Programming Languages and Operating Systems*, New York, NY, USA, Apr., 2017, p. 615–629.
- [33] C. Hu, W. Bao, D. Wang, and F. Liu, “Dynamic adaptive DNN surgery for inference acceleration on the edge,” in *IEEE INFOCOM 2019 - IEEE Conference on Computer Communications*, Paris, France, Jun., 2019, pp. 1423–1431.
- [34] Y. Xiao, L. Xiao, K. Wan, H. Yang, Y. Zhang, Y. Wu, and Y. Zhang, “Reinforcement learning based energy-efficient collaborative inference for mobile edge computing,” *IEEE Transactions on Communications*, vol. 71, no. 2, pp. 864–876, Feb. 2023.
- [35] P. Liang, Y. Tang, X. Zhang, Y. Bai, T. Su, Z. Lai, L. Qiao, and D. Li, “A survey on auto-parallelism of large-scale deep learning training,” *IEEE Transactions on Parallel and Distributed Systems*, vol. 34, no. 8, pp. 2377–2390, Aug. 2023.
- [36] W. Wei, J. Wang, Z. Fang, J. Chen, Y. Ren, and Y. Dong, “3u: Joint design of UAV-USV-UUV networks for cooperative target hunting,” *IEEE Transactions on Vehicular Technology*, vol. 72, no. 3, pp. 4085–4090, Mar., 2023.
- [37] W. Wei, J. Wang, J. Du, Z. Fang, Y. Ren, and C. L. P. Chen, “Differential game-based deep reinforcement learning in underwater target hunting task,” *IEEE Transactions on Neural Networks and Learning Systems*, vol. 36, no. 1, pp. 462–474, Jan., 2025.
- [38] W. Wei, J. Wang, J. Du, Z. Fang, C. Jiang, and Y. Ren, “Underwater differential game: Finite-time target hunting task with communication delay,” in *IEEE International Conference on Communications*, Seoul, Korea, May, 2022, pp. 3989–3994.
- [39] Z. Wang, Z. Zhang, J. Wang, C. Jiang, W. Wei, and Y. Ren, “AUV-assisted node repair for iout relying on multiagent reinforcement learning,” *IEEE Internet of Things Journal*, vol. 11, no. 3, pp. 4139–4151, Feb., 2024.
- [40] S. Li and T. Hoefler, “Chimera: Efficiently training large-scale neural networks with bidirectional pipelines,” in *Proceedings of the International Conference for High Performance Computing, Networking, Storage and Analysis*. New York, NY, USA: Association for Computing Machinery, Nov., 2021, pp. 1–14.
- [41] A. Kosson, V. Chiley, A. Venigalla, J. Hestness, and U. Köster, “Pipelined backpropagation at scale: Training large models without batches,” *arXiv preprint arXiv:2003.11666*, Apr., 2021.
- [42] W. Zhou, Z. Qu, Y. Zhao, B. Tang, and B. Ye, “An efficient split learning framework for recurrent neural network in mobile edge environment,” in *Proceedings of the Conference on Research in Adaptive and Convergent Systems*, New York, NY, USA, Oct., 2022, p. 131–138.
- [43] S. Fan, Y. Rong, C. Meng, Z. Cao, S. Wang, Z. Zheng, C. Wu, G. Long, J. Yang, L. Xia, L. Diao, X. Liu, and W. Lin, “DAPPLE: A pipelined data parallel approach for training large models,” in *Proceedings of the ACM SIGPLAN Symposium on Principles and Practice of Parallel Programming*. New York, NY, USA: Association for Computing Machinery, Feb. 2021, p. 431–445.
- [44] Y. Tian, Z. Zhang, Z. Yang, and Q. Yang, “JMSNAS: Joint model split and neural architecture search for learning over mobile edge networks,” *arXiv preprint arXiv:2111.08206*, 2021.
- [45] J. Tirana, S. Lalis, and D. Chatzopoulos, “MP-SL: Multihop parallel split learning,” *arXiv preprint arXiv:2402.0020*, 2024.
- [46] Z. Lin, G. Zhu, Y. Deng, X. Chen, Y. Gao, K. Huang, and Y. Fang, “Efficient parallel split learning over resource-constrained wireless edge networks,” *IEEE Trans. Mobile Comput.*, pp. 1–16, early access, 2024.
- [47] J. Ren, G. Yu, and G. Ding, “Accelerating DNN training in wireless federated edge learning systems,” *IEEE Journal on Selected Areas in Communications*, vol. 39, no. 1, pp. 219–232, Nov. 2021.
- [48] Z. Lin, G. Qu, W. Wei, X. Chen, and K. K. Leung, “Adaptsfl: Adaptive split federated learning in resource-constrained edge networks,” *arXiv preprint arXiv:2403.13101*, 2024.
- [49] G. Yeung, D. Borowiec, R. Yang, A. Friday, R. Harper, and P. Garaghan, “Horus: Interference-aware and prediction-based scheduling in deep learning systems,” *IEEE Transactions on Parallel and Distributed Systems*, vol. 33, no. 1, pp. 88–100, Jan. 2022.
- [50] V. Cacchiani, M. Iori, A. Locatelli, and S. Martello, “Knapsack problems — an overview of recent advances. part II: Multiple, multidimensional, and quadratic knapsack problems,” *Computers & Operations Research*, vol. 143, p. 105693, Feb. 2022.
- [51] H. He, H. Daumé, and J. Eisner, “Learning to search in branch-and-bound algorithms,” in *Proceedings of the International Conference on Neural Information Processing Systems*. Montreal, Canada: MIT Press, Dec., 2014, p. 3293–3301.
- [52] M. Minoux, “Solving combinatorial problems with combined min-max-min-sum objective and applications,” *Mathematical Programming*, vol. 45, pp. 361–372, Aug. 1989.
- [53] B. Haeupler, R. Hladík, V. Rozhoň, R. Tarjan, and J. Tětek, “Universal optimality of Dijkstra via beyond-worst-case heaps,” *arXiv preprint arXiv:2311.11793*, 2024.
- [54] A. Frieze and J. Yadegar, “On the quadratic assignment problem,” *Discrete Applied Mathematics*, vol. 5, no. 1, pp. 89–98, Sep., 1983.
- [55] Gurobi Optimization, LLC, “Gurobi Optimizer Reference Manual,” 2024. [Online]. Available: <https://www.gurobi.com>
- [56] P. Tseng, “Convergence of a block coordinate descent method for nondifferentiable minimization,” *J Optim Theory Appl*, vol. 109, pp. 475–494, Jun. 2001.
- [57] L. Grippo and M. Sciandrone, “On the convergence of the block nonlinear gauss–seidel method under convex constraints,” *Oper. Res. Lett.*, vol. 26, no. 3, pp. 127–136, Apr., 2000.
- [58] Z. Lin, G. Zhu, Y. Deng, X. Chen, Y. Gao, K. Huang, and Y. Fang, “Efficient parallel split learning over resource-constrained wireless edge networks,” *IEEE Transactions on Mobile Computing*, vol. 23, no. 10, pp. 9224–9239, Jan., 2024.
- [59] X. Hu, L. Wang, K.-K. Wong, M. Tao, Y. Zhang, and Z. Zheng, “Edge and central cloud computing: A perfect pairing for high energy efficiency and low-latency,” *IEEE Trans. Wireless Commun.*, vol. 19, no. 2, pp. 1070–1083, Feb., 2019.
- [60] M. K. Samimi, T. S. Rappaport, and G. R. MacCartney, “Probabilistic omnidirectional path loss models for millimeter-wave outdoor communications,” *IEEE Wireless Commun. Lett.*, vol. 4, no. 4, pp. 357–360, Aug., 2015.
- [61] Y. Lecun, L. Bottou, Y. Bengio, and P. Haffner, “Gradient-based learning applied to document recognition,” *Proc. IEEE*, vol. 86, no. 11, pp. 2278–2324, Nov. 1998.
- [62] W. J. Robinson M., F. Esposito, and M. A. Zuluaga, “DTS: A simulator to estimate the training time of distributed deep neural networks,” in *International Symposium on Modeling, Analysis, and Simulation of Computer and Telecommunication Systems*, Nice, France, March 2023, pp. 17–24.
- [63] Y. Yoo and S. Jung, “Modeling forecast errors for microgrid operation using Gaussian process regression,” *Scientific Reports*, vol. 14, no. 1, p. 2166, Jan., 2024.